Deep Learning Based Processing of EEG Signals for Detection and Recognition of Alzheimer Disease

Uğur Aydın Türeli

Submitted to the
Institute of Graduate Studies and Research
in partial fulfillment of the requirements for the degree of

Master of Science
in
Computer Engineering

Eastern Mediterranean University
January 2023
Gazimağusa, North Cyprus

Approval of the Institute of Graduate Studies and Research

Prof. Dr. Ali Hakan Ulusoy
Director

I certify that this thesis satisfies all the requirements as a thesis for the degree of Master of Science in Computer Engineering.

Prof. Dr. Zeki Bayram
Chair, Department of Computer Engineering

We certify that we have read this thesis and that in our opinion it is fully adequate in scope and quality as a thesis for the degree of Master of Science in Computer Engineering.

Assoc. Prof. Dr. Adnan Acan
Supervisor

Examining Committee

1. Assoc. Prof. Dr. Adnan Acan

2. Assoc. Prof. Dr. Mehtap Köse Ulukök

3. Asst. Prof. Dr. Ahmet Ünveren

ABSTRACT

The aim of this study is to provide early diagnosis of Alzheimer's disease (AD). Two-dimensional color image transformations of EEG signals will be processed for early diagnosis.

Alzheimer's disease; It is a common type of dementia neurological disease that occurs in advanced ages and causes a decrease in thought, memory and behavioral functions. There is no definitive cure for Alzheimer's disease. However, it is possible to both slow down the process and reduce the severity of some symptoms. For this, early and accurate diagnosis is of great importance.

EEG data were obtained from the dataset of 88 participants (35 healthy people, 31 with mild Alzheimer's disease and 22 with Alzheimer's disease) Alzheimer's disease and healthy people. EEG signals converted to Gramian Summation Angular Field images were firstly processed through various preprocessing steps.

The 2D color image data obtained was trained and tested using the AlexNet deep learning model. AlexNet, a Convolutional Neural Network model, consists of 8 layers. In the literature review, 16 channels were selected in various studies and the 3 channels with the highest results were used. The same channels were also selected for this study. Among these channels, F7, T3 and T5 channels have the highest success rate. The three channels with the highest results were used in this study.

GASF images of selected F7, T3 and T5 channels were used to train the AlexNet CNN model over 50 epochs. The developed model achieved promising performance with

98.03% accuracy, 98.21% sensitivity and 97.84% specificity. In addition, the AlexNet CNN model was trained and tested over 50 epochs with 4-fold Cross Validation.

As a result of this study, the developed model achieved the highest results with 98.02% accuracy, 98.01% sensitivity and 98.04% specificity.

Keywords: alzheimer disease, deep learning, eeg, gasf, cnn.

ÖZ

Bu çalışmanın amacı Alzheimer hastalığının (AD) erken teşhisini sağlamaktır. Erken teşhis için EEG sinyallerini iki boyutlu renkli görüntü dönüşümleri işlenecektir.

Alzheimer hastalığı; düşünce, hafıza ve davranış fonksiyonlarında azalmaya neden olan ve ileri yaşlarda ortaya çıkan yaygın olarak görülen bir demasn türü nörolojik bir hastalıktır. Alzheimer hastalığının kesin bir tedavisi yoktur. Fakat hem süreci yavaşlatmak hem de kimi belirtilerin şiddetini azaltmak mümkündür. Bunun için de erken ve doğru tanı büyük önem taşır.

EEG verileri, Alzheimer hastalığı olan ve sağlıklı olan 88 katılımcının (35 sağlıklı, 31 hafif Alzheimer hastalığı ve 22 Alzheimer hastalığı) veri setinden elde edildi. Gramian Summation Angular Field görüntülerine dönüştürülen EEG sinyalleri öncelikle çeşitli ön işleme adımlarından geçirilmiştir.

Elde edilen 2B renkli görüntü verilerini AlexNet derin öğrenme modeli kullanılarak eğitilmiş ve test edilmiştir. Evrişimsel Sinir Ağı modeli olan AlexNet 8 katmandan oluşur. Literatür taramasında çeşitli çalışmalarda 16 kanal seçilmiş ve en yüksek sonuç veren 3 kanal kullanılmıştır. Aynı kanallar bu çalışma için de seçilmiştir. Bu kanallar ara sında F7, T3 ve T5 kanalları başarı oranı en yüksek olan kanallardır. bu çalışmada en yüksek sonuç veren üç kanal kullanılmıştır.

Seçilen F7, T3, T5 kanallarının GASF görüntüleri, AlexNet CNN modelini 50 dönemin üzerinde eğitmek için kullanıldı. Geliştirilen model %98,03 doğruluk, %98,21 duyarlılık ve %97,84 özgüllük ile umut verici bir performans elde etmiştir. Ek

olarak, AlexNet CNN modeli 4-kat Çapraz Doğrulama ile 50 dönemin üzerinde eğitildi ve test edildi.

Bu çalışma sonucunda geliştirilen model %98,02 doğruluk, %98,01 duyarlılık ve %98.04 özgüllük ile en yüksek sonuçlara ulaşmıştır.

Anahtar Kelimeler: alzheimer hastalığı, derin öğrenme, eeg, gasf, cnn.

DEDICATION

To my family

ACKNOWLEDGMENT

I would like to record my gratitude to Assoc. Prof. Dr. Adnan ACAN for his supervision, advice, and guidance from the very early stage of this thesis as well as giving me extraordinary experiences throughout the work. Above all and the most needed, he provided me constant encouragement and support in various ways. His ideas, experiences, and passions has truly inspire and enrich my growth as a student. I am indebted to him more than he knows.

TABLE OF CONTENTS

LIST OF TABLES

LIST OF FIGURES

LIST OF ABBREVIATIONS

AD	Alzheimer's Disease
ANN	Artificial Neural Network
CNN	Convolutional Neural Network
EEG	Electroencephalogram
GADF	Gramian Difference Angular Field
GAF	Gramian Angular Field
GASF	Gramian Summation Angular Field
LSSVM	Least Squares Support Vector Machine Classifiers
NS	Health Control
RNN	Recurrent Neural Network

Chapter 1

INTRODUCTION

1.1 Alzheimer's Disease

Alzheimer's disease is a common type of dementia, a progressive neurological disease that causes the destruction of brain cells. In this disease, which causes a decrease in thought, memory and behavioral functions, the symptoms appear gradually with age. Alzheimer's disease can take years to reach advanced stages. Since it is a progressive disease, early symptoms in Alzheimer's disease are usually seen as forgetting recent events, but within a few years, individuals may have difficulty in performing their daily activities on their own. Social skills, behaviors, and the ability to think logically are also negatively affected over time.

Advanced-stage Alzheimer's patients often lose the ability to have a conversation with a person and begin to have difficulty in responding to the questions asked and the events surrounding them. Alzheimer's disease is a neurodegenerative disease that mostly occurs with old age [1], [2]. Today, people aged 65 and over constitute the fastest growing age group all over the world (especially in developed countries and welfare societies). The incidence of Alzheimer's disease increases with age (8 out of 100 people over the age of 65 have Alzheimer's disease).

While 50 million people worldwide were affected by Alzheimer's disease in 2018, it is predicted that this figure will be 82 million in 2030 and will increase depending on

time [3]. If natural, social or economic disasters are not encountered in the 21st century, the incidence of Alzheimer's disease will increase even more. As a result of thinning of the brain tissue, it shows symptoms as disorders in memory, speech and motor skills. Behavior and thinking skills are affected in Alzheimer's disease and gradually regress during the stages of Alzheimer's disease.

Alois Alzheimer was a German neuropsychiatrist who first described Alzheimer's disease. In 1902, 51-year-old Auguste Deter was admitted by his wife to Dr. brought to Alzheimer's. Examining and following the patient, Dr. Alzheimer's performs an autopsy following the death of the patient in 1906. In the brain samples he took, thinning of the patient's cortex and different accumulations in and around the cells are encountered. This invention of Alzheimer's, which defines plaque and fiber, was presented in medical congresses in the following years and is known as Alzheimer's disease[3].

Alzheimer's disease is a progressive neurocognitive disorder that worsens over time. Alzheimer's mainly affects the elderly and usually progresses within a few years. Gradual memory loss may occur, as well as changes in behavior, thinking, and language skills. Although each person with Alzheimer's experiences the disease differently, it is possible to examine its progression typically in stages. Looking at Alzheimer's disease in stages can provide a clearer idea of possible changes that may affect a person after diagnosis. Usually the houses of Alzheimer's disease are examined in five phase [3].

Phase 1 :

Preclinical Alzheimer's disease. Functional changes due to this long-stage Alzheimer's disease, called pre-clinical, may begin years before the disease is diagnosed. At this stage, an excess of a protein called amyloid beta is usually detected. Other than that, there are no specific symptoms. Also, at this stage, the patient has no clinical symptoms. In people with Alzheimer's disease, this protein clumps together and forms plaques. These protein clumps can block cell-to-cell signaling and activate immune system cells that trigger inflammation. Other biomarkers or biomarkers can indicate whether a person is more likely to develop Alzheimer's symptoms. Genetic testing can also detect a higher risk.

Phase 2 :

Mild cognitive impairment. Forgetfulness can be caused by both Alzheimer's disease and advanced age. But not all older people develop dementia. Mild cognitive impairment is a more significant cognitive decline than forgetfulness that occurs as a normal part of aging. People often have trouble remembering current events, conversations, or things to do. However, there is no forgetfulness that is strong enough to have problems in daily life activities. It is normal for individuals to be unable to remember or forget things as they get older. However, if the person has started to experience forgetfulness that will cause problems in his daily life routine, if he has difficulty in making decisions, if he has become more impulsive, if there is irritability, aggression, apathy and anxiety, these may be symptoms.

Phase 3 :

Slight forgetfulness. The stage at which Alzheimer's disease is usually diagnosed is mild dementia. At this stage, the Alzheimer's patient begins to have problems with

thinking and memory. These problems have become more noticeable by the people around them. Symptoms of mild dementia due to Alzheimer's disease can be summarized as not being able to use the right words, getting lost, putting an item in the wrong place, having difficulty choosing the right word, being angry, low motivation, having problems completing tasks, having difficulty remembering, asking the same questions again, or having problems solving problems.

Phase 4 :

Moderate forgetfulness. If a patient is an Alzheimer's patient with moderate dementia, they become more forgetful and more confused. Because of this, they may need help taking care of themselves and with daily tasks. The main symptoms of moderate dementia due to Alzheimer's disease are as follows: needing help, hearing or seeing things that are not there, excessive suspicion of friends or family, physical outbursts that may be aggressive, not remembering seasons or days, confusing strangers with family members or close friends, forgetting roads, forgetting phone number or address information.

Phase 5 :

Severe forgetfulness: At this stage, the Alzheimer's patient will need more care and assistance, as he will not be able to perform his daily tasks. While the loss of mental strength continues at this stage, there may be limitations in movement and physical abilities. Symptoms may also include: inability to speak/communicate coherently, need full assistance with self-care, eating, dressing, and bathing, inability to sit up/hold head/walk unaided, stiff muscles and abnormal reflexes, loss of swallowing ability, bladder and inability to control bowel movements. A person with severe Alzheimer's disease is more likely to develop pneumonia. Pneumonia is common in Alzheimer's

patients because of loss of ability to swallow, food and drink that can get into the lungs and cause infection. These individuals are at high risk of inadequate water and nutrient intake and require careful attention.

1.1.1 Diagnostic Methods of Alzheimer's Disease

There is no differential diagnostic test that can provide clear information for the diagnosis of Alzheimer's disease. Therefore, many medical diagnostic tests are evaluated together in the diagnosis of the disease. Patients who apply to health institutions with symptoms related to the disease are directed to neurology clinics. First of all, a detailed history of the patient is taken by neurologists. At this stage, it may be necessary to ask some questions to the family or close circle of the patient as well as the patient. After the medical history is taken, various scans are performed to measure neurological functions, balance, sensation, behavior, memory and reflexes. Applications such as blood tests, ultrasonography, computed tomography (CT), electroencephalography (EEG), magnetic resonance imaging (MR) and personality screening tests to investigate depression can also be applied to support the diagnosis and rule out the possibility of similar diseases.

EEG signals are an important tool widely used in the study of brain functions. EEG signals have been widely used in the development of computer-assisted diagnostic systems aimed at diagnosing many diseases due to the lower cost and lower time requirement compared to other biomedical imaging methods (such as CT-Computed Tomography, MRIMagnetic Resonance Imaging, PET- Positron Emission Tomography, fMRI - Functional Magnetic Resonance Imaging). is preferred.

1.1.2 Treatment in Alzheimer's Disease

There is no definitive treatment for Alzheimer's disease, but with medication, symptomatic treatment and behavioral practices, it can be helped to reduce the problems that occur in the understanding and comprehension ability of the Alzheimer's disease and behavioral symptoms (dressing, eating, teeth, bathroom, hygiene, getting to know their relatives). Once you are definitively diagnosed as Alzheimer's disease by experts, the treatment process begins. This process may vary from person to person, depending on the age of the patient and the level of Alzheimer's disease. There are certain medications and practices to soothe some of the symptoms caused by Alzheimer's disease. Some of the practices in question are making changes that will make it easier to move around in the home environment or leaving memories triggering objects and notes in order to ensure that Alzheimer's disease live as independently as possible.

Psychological treatment modalities, such as cognitive stimulation therapy, may benefit the patient's memory, problem-solving ability, and speech. Drugs approved by the American Food and Drug Administration (FDA) are frequently used in moderate Alzheimer's diseases and severe Alzheimer's disease. These drugs are given under physician supervision to reduce symptoms and relieve behavioral distress caused by Alzheimer's disease. These drugs, which work on the principle of managing neurotransmitters, which are chemicals that transmit messages between neurons, can work and reduce symptoms in most patients, although they do not resolve the underlying cause of Alzheimer's disease.

1.2 Literature Review

In this section, a literature review will be conducted on Methods of Displaying Time Series to Improve Classification, deep learning approaches for electroencephalogram analysis based on gramian angular field transform.

Huggins et al. Deep learning of resting-state electroencephalogram signals for three-class classification of Alzheimer's disease, mild cognitive impairment and healthy ageing [4].

In this study, a deep learning model is proposed for the diagnosis of Alzheimer's disease. This model was trained and tested with EEG recordings of healthy participants and Alzheimer's patients. The dataset used in this study was obtained from the Department of Neurology at Hospital das Clinicas in Sao Paulo, Brazil. The dataset used was collected with a Braintech 3.0 EEG device with a sampling frequency of 200 Hz. Records were collected in 21 channels with the Braintech EEG device used while creating the data set. These records are listed below.

• Fp1,	• Fz,	• P4,	• F7,	• T6
• Fp2,	• C3,	• Pz,	• F8,	
• Fpz,	• C4,	• O1,	• T3,	
• F3,	• Cz,	• O2,	• T4,	
• F4,	• P3,	• Oz,	• T5,	

The dataset was collected from 141 subjects in total. The dataset consists of three parts. The first of these fragments was collected from 52 AD (Alzheimer's disease) subjects. These subjects are individuals between the ages of 77.6 - 87.0. The second piece of dataset was collected from 37 MCI(mild cognitive impairment) subjects. These subjects are individuals between the ages of 73.3 and 83.5 years. The third part of the dataset was collected from 52 HA(healthy aging) subjects. These subjects are individuals between the ages of 73.6 and 85.6. All obtained data were preprocessed. Samples for each channel in the dataset were divided into 5 seconds of sampling time. Time-frequency maps were generated for each sample of each electrode using CWT (continuous wavelet transform). A total of 340,137 images were obtained using CWT.

An example CWT image is presented below.

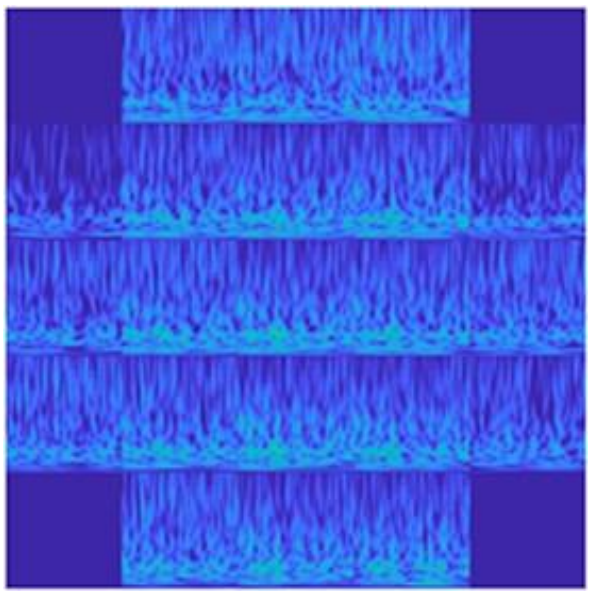

Figure 1: Example CWT image

All obtained images were trained and tested with AlexNet CNN architecture. AlexNet CNN architecture consists of 8 layers in total. Of these layers, 5 are convolutional layers and 3 are fully connected layers.

In addition, K-Fold Cross-Validation is used in the training and testing process. The K value was selected as 10 and retrained and tested.

Confusion Matrices and (ROC) receiver operating characteristic curves were generated to evaluate the performance of the proposed model.

The results obtained with 10-Fold Cross Validation range from 98.5% to 99.3%.

This study yielded promising results. However, it is stated in the article that more studies are needed to further this research.

Fiscon et al. Alzheimer’s disease patients classification through EEG signals processing [5].

The aim of this study is to classify EEG biomedical signals consisting of AD MCI and CT datasets with machine learning methods. Given IRCCS Centro Neurolesi Bonino-Pulejo was taken. (AD) represents Alzheimer's Disease participants. (MCI) represents the participants of the Mild Cognitive Impairment. (CT) represents healthy controls participants. AD participants are individuals between the ages of 72.0 and 84.8. MCI participants are individuals aged 64.7 to 83.5 years. CT participants are individuals between the ages of 54.7 and 73.5 years. Of the 86 AD participants, 49 participants

were female and 37 participants were male. CT participants consist of 5 female and 9 male participants.

The following electrodes were used in data preprocessing.

• Fp1	• Fz	• C3	• T5	• T6
• Fp2	• F4	• Cz	• P3	• O1
• F7	• F8	• C4	• Pz	• O2
• F3	• T3	• T4	• P4	

The data were kept in 300 second recordings at 256 and 1024 sampling frequencies. Participants were asked to keep their eyes closed while recording. Fast Fourier Transform functions (FFT) were used by performing MATLAB R spectral analysis. In this study, Support Vector Machines (SVM), Decision Trees, Rule-based classifiers were used respectively for classification. Accuracy (A), Precision (P), Recall (R), Specificity (S), and F-measure (F) were calculated to evaluate classification performance. The classification performance of 3 different datasets in different variations was tested. Obtained results are presented in the table below.

Table 1: Table of results [5]

Sampling	AD *vs* CT			MCI *vs* CT			AD *vs* MCI		
	SVM	J48	DMB	SVM	J48	DMB	SVM	J48	DMB
Accuracy	54	**86**	62	51	**88**	61	49	**83**	51
Precision	62	**85**	57	59	**88**	57	49	**83**	50
Recall	54	**86**	62	51	**88**	61	49	**83**	51
Specificity	36	60	18	46	**82**	32	47	**81**	48
F-measure	57	**85**	59	54	**88**	59	49	**82**	50

In the results obtained, it has been shown that Decision Tree methods give better results than other methods in terms of classification performance. In future studies, it is aimed to use Wavelet Transform for better classification of the dataset.

Zhao et al. Deep Learning in the EEG Diagnosis of Alzheimer's Disease [6].

In this study, it is aimed to classify Alzheimer's disease using electroencephalogram (EEG) recordings. The EEG dataset used in this study was collected from 15 Alzheimer's patients and 15 healthy people. Recordings from each participant were collected from 16 electrodes. These 16 electrode names are listed below.

Fp1, Fp2, Fz, F3, F4, F7, F8, C3, C4, Pz, P3, P4, T5, T6, O1 and O2.

EEG recordings consist of recordings of approximately 20 minutes each. It has a bandpass of 0.530 Hz.

In this study, a literature review was conducted. In the scan, the data were preprocessed with some thresholds and filters to remove the noise before the train and test of the EEG data. Then, a deep learning network was created to classify the data. The input layer of the deep learning network has been changed to make it more suitable for EEG

data. During the experiment, it was aimed to create the best deep learning network by using different numbers of nodes and hidden layers. Finally, 16 electrodes were combined in order to get better results. As a result, the SVM model trained using all electrodes of a person achieved 92% accuracy.

Acharya et al. Deep convolutional neural network for the automated detection and diagnosis of seizure using EEG signals [7].

The aim of this study is to diagnose Alzheimer's disease using convolutional neural networks (CNN) deep learning model. EEG dataset is used in this study. The dataset used in this study was obtained from Andrzejak et al. at Bonn University, Germany. The dataset consists of 3 parts. These pieces are Set B, Set D, and Set E. Set B represents regular participants. Set D represents preictal participants. Set D represents seizure participants. Each dataset contains 100 EEG signals and is a 23.6-second recording consisting of a single channel. Each Set (B,D,E) consists of 5 subjects containing 100 cases. EEG signals were normalized with Z-score normalization, zero mean and standard deviation of 1 for training and testing, respectively, and the sampling rate was 173.61 Hz. In this study, the 3-layer CNN model was used. These layers are respectively; Convolutional layer, Pooling layer and Fully connected layer. This model is trained over 150 periods. While the model is being trained, 70% of the entire dataset is reserved as a train. The remaining 30% is reserved for testing. In addition, k-fold cross-validation was applied in this study. The K value was selected as 10 and retrained and tested. The MATLAB program was used for the proposed CNN model and each train process was completed in approximately 12.8 seconds. Suggested CNN model; It consists of a total of 13 layers consisting of Convolutional layer, Pooling layer and Fully connected layer. As a result, 88.7% accuracy, 90% specificty

and 95% sensitivity results were obtained in the classification of Alzheimer's disease with the deep learning-based CNN algorithm. To improve the performance of the technique used, it is necessary to increase the bagging algorithm and the number of samples. The scores obtained in this study were compared with different studies. It has been observed that the results obtained using CNN give high results according to some studies and low results according to some studies. It is stated in this study that the proposed technique should be trained and tested with larger EEG datasets in order to give better results.

Chapter 2

ELECTROENCEPHALOGRAPHY

There are billions of nerve cells in the nervous systems of the human body. Most of these nerve cells are in the brain. Cells in the brain are in constant communication with each other. This communication leads to an electrical activity. There are recording devices used to measure these electrical activities. Recordings called electroencephalogram or EEG can be recorded with a recording device called Electroencephalography. This technique, developed by the German physician Hans Berger in 1929, is called EEG.

Electroencephalography (EEG) is the name given to the method of recording the electrical activity in the brain of electrodes attached to the scalp. Using these electrodes, which detect low-voltage electrical signals, the electrical activity in every part of the brain can be easily recorded. Electrodes are small flat pieces of metal. The electrodes are attached to the scalp via a conductive gel. EEG waves can fluctuate, and doctors examining these recordings can tell if there is an abnormal signal when they look at the recording lines. Irregular fluctuations in waves are interpreted as abnormal conditions. EEG is most commonly used in the diagnosis of epilepsy. However, it is also used in other neurological disorders such as Parkinson's and Alzheimer's diseases. No electric current is given to the patient during the EEG procedure and the patient does not feel any pain during the EEG recording.

Since the EEG test does not have any side effects, it can be applied to people of all age groups. In addition, there is no danger in its application to children and pregnant women. Generally, 3 different activities can be requested from the patient while taking EEG recordings. These could be staring at a steady light, breathing fast, or blinking for 3 minutes. The EEG test, called routine EEG, is done for a short time while awake.

However, abnormal electrical activity that is not visible in a routine EEG test may occur during sleep. Therefore, EEG recordings can also be made while asleep. This is because some epileptic seizures occur only during sleep. The EEG recording, which is accepted as the correct technique, is the recordings taken both while awake and during sleep. The name of the recordings taken in this way is called "sleep-wake EEG". There are many external factors that affect EEG recordings. For example, the patient's hair being dirty or not lying in a comfortable position may positively or negatively affect the quality of the EEG recording.

Before the EEG recording starts, some operations are performed by the technician. First of all, after the head measurement is made, the places where the electrodes will be attached are determined. A gel is used for conductivity before the electrodes are attached to the scalp. While a minimum of 12 electrodes can be used to take EEG recordings, a maximum of 64 electrodes can be used. Below is an EEG-Cap image. It is possible to make more precise measurements using EEG - Cap.

Figure 2: EEG – Cap [8]

Each electrode is called a channel, and each channel has a name. The most commonly used of these channels are C3, C4, Cz, F3, F4, F7, F8, FP1, FP2, Fz, O1, O2, Oz, P3, P4, Pz, T3, T4, T5 and T6. The anterior and posterior parts of the skull are identified as Nasion and Inion. The nasion represents the front of the skull. Inion refers to the back of the skull. When sticking the electrodes, care should always be taken to stick them in the same place. Below are images of two different, simple and detailed electrode designs.

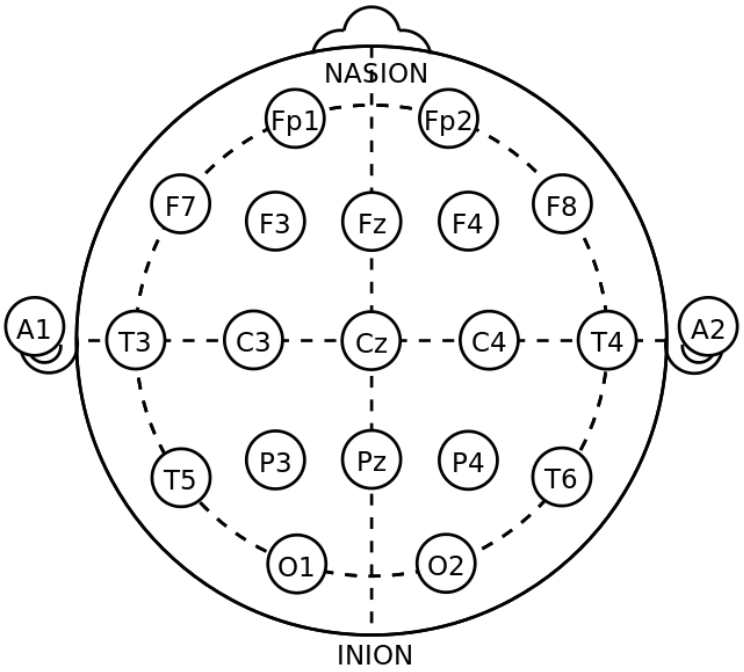

Figure 3: EEG simple electrode layouts[9]

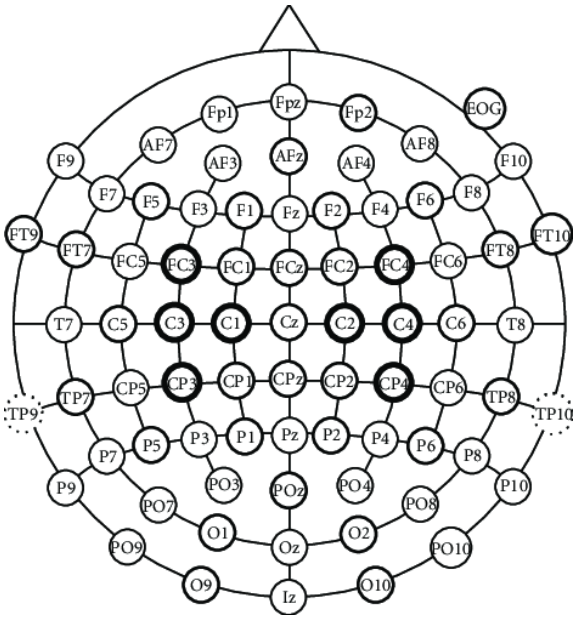

Figure 4: EEG detailed electrode layouts[10]

After all the electrodes are connected to the computer. When recording begins, electrical activity in the brain begins to be recorded on a storage device.

It ensures that the patient is in a comfortable position during recording. While these recordings are being taken, the patient may be asked to do simple math or look at a picture to increase the electrical activity in the brain.

During the EEG test, different frequencies can be recorded. There are many different types of frequencies, from 0 to 100 Hz. Such frequencies and Hz ranges are listed in the table below.

Table 2: EEG test different frequency ranges

Type	F**requency** (Hz)	Operation
Delta	0,5-3.5 Hz	In adults; Occurs in sleep mode.
Teta	4-7 Hz	In adults; arousal, laziness
Alfa	8-12 Hz	comfortable reflection close eyes
SMR	12-15 Hz	SMR
Beta	12-38 Hz	in alert work, busy, active or anxious thinking, effective concentration
Beta (Middle)	15-21 Hz	in alert work, busy, active or anxious thinking, effective concentration, normal concentration
Beta (High)	21-38 Hz	Stress, anxiety
Gamma	34-100+ Hz	certain motor brain functions

When the results of the EEG test are completed, evaluations are made taking into account the drugs used and the age of the patient. Only a neurologist can make these assessments. If the patient has a previous EEG test, the results of the old test and the new test are compared. If it is observed that the electrical activity in the brain is not in harmony, it is concluded that there may be a health problem related to the brain. Then, the disease caused by this incompatible electrical activity is determined by the relevant specialists by applying different tests.

Chapter 3

CONVOLUTIONAL NEURAL NETWORKS

With the latest developments in artificial intelligence, deep learning models that can perceive and classify like humans continue to develop day by day. Convolutional Neural Networks (CNN) is one of the most widely used deep learning-based algorithms for image classification and detection. Convolutional Neural Networks is a deep learning algorithm consisting of layers, Convolutional Layer (Relu), Pooling and Fully Connected layers.

ALexNet is a CNN architecture developed in 2012 by Alex Krizhevsky, Ilya Sutskever and Geoffrey Hinton. The 8-layer AlexNet architecture has proven itself by getting high results in the ImageNet Large-Scale Image Recognition Competition [11]. AlexNet was successful in the competition with an error rate of 15.3%. Of the 8 layers, 5 are "convolutional layers" and 3 are "fully connected" layers. The following image shows the AlexNet architecture.

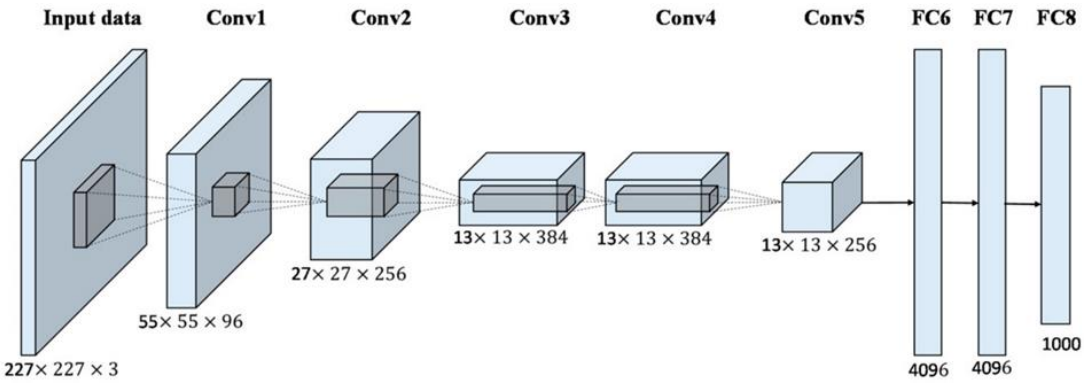

Figure 5: AlexNet architecture [12]

AlexNet has a very similar structure to the LeNet architecture. [13] However, there are important differences. AlexNet architecture is much deeper than LeNet, while AlexNet consists of 8 layers, LeNet consists of 5 layers. AlexNet can show different actions in non-linear situations. Most standard neural networks used tanh or sigmoid. AlexNet uses ReLU as activation function instead of tanh or sigmoid. ReLU is more advantageous than sigmoid. It is advantageous because the model is faster when being trained.

AlexNet contains eight layers with weights; the first five are convolutional and the remaining three are fully- connected. The output of the last fully-connected layer is fed to a 1000-way softmax which produces a distribution over the 1000 class labels. Our network maximizes the multinomial logistic regression objective, which is equivalent to maximizing the average across training cases of the log-probability of the correct label under the prediction distribution. The kernels of the second, fourth, and fifth convolutional layers are connected only to those kernel maps in the previous layer which reside on the same GPU. The kernels of the third convolutional layer are connected to all kernel maps in the second layer. The neurons in the fully- connected layers are connected to all neurons in the previous layer. Response-normalization

layers follow the first and second convolutional layers. The ReLU non-linearity is applied to the output of every convolutional and fully-connected layer.

The first convolutional layer filters the 224 × 224 × 3 input image with 96 kernels of size 11 × 11 × 3 with a stride of 4 pixels (this is the distance between the receptive field centers of neighboringAn illustration of the architecture of our CNN, explicitly showing the delineation of responsibilities between the two GPUs. One GPU runs the layer-parts at the top of the figure while the other runs the layer-parts at the bottom. The GPUs communicate only at certain layers. The network's input is 150,528-dimensional, and the number of neurons in the network's remaining layers is given by 253,440–186,624–64,896–64,896–43,264– 4096–4096–1000. neurons in a kernel map). The second convolutional layer takes as input the (response-normalized and pooled) output of the first convolutional layer and filters it with 256 kernels of size 5 × 5 × 48. The third, fourth, and fifth convolutional layers are connected to one another without any intervening pooling or normalization layers. The third convolutional layer has 384 kernels of size 3 × 3 × 256 connected to the (normalized, pooled) outputs of the second convolutional layer. The fourth convolutional layer has 384 kernels of size 3 × 3 × 192 , and the fifth convolutional layer has 256 kernels of size 3 × 3 × 192. The fully-connected layers have 4096 neurons each.

As indicated in the image below, as the values of the sigmoid function get larger or smaller, its derivative approaches zero. This situation is called vanishing gradient. In this case, it becomes very difficult to update the weights. In deep models, this makes learning difficult.

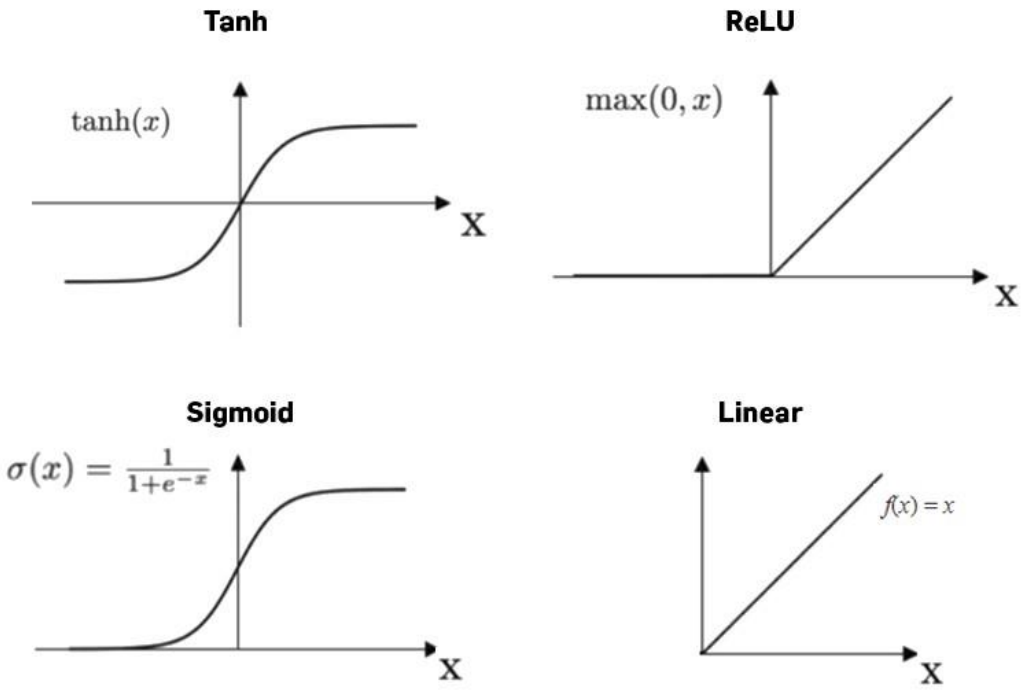

Figure 6: Tanh, ReLU, sigmoid, linear coordinate plane [14]

Another advantage of the AlexNet architecture is to avoid overfitting by using dropout. Overfitting is the memorization of the data given to the model for the train by the model. This problem can be summarized as training accurucy giving 99.5% and test accuracy 75.0%. In this case, it means that the model has not learned the data given for the train and has memorized it. AlexNet has prevented this by using dropout.

AlexNet consists of many parameters in total. Images can be given to the input layer of the network, such as 128x128x3 for example. The 3 here means RGB. The table below presents a table with AlexNet's layers and number of parameters.

AlexNet Network - Structural Details													
Input			Output			Layer	Stride	Pad	Kernel size		in	out	# of Param
227	227	3	55	55	96	conv1	4	0	11	11	3	96	34944
55	55	96	27	27	96	maxpool1	2	0	3	3	96	96	0
27	27	96	27	27	256	conv2	1	2	5	5	96	256	614656
27	27	256	13	13	256	maxpool2	2	0	3	3	256	256	0
13	13	256	13	13	384	conv3	1	1	3	3	256	384	885120
13	13	384	13	13	384	conv4	1	1	3	3	384	384	1327488
13	13	384	13	13	256	conv5	1	1	3	3	384	256	884992
13	13	256	6	6	256	maxpool5	2	0	3	3	256	256	0
						fc6			1	1	9216	4096	37752832
						fc7			1	1	4096	4096	16781312
						fc8			1	1	4096	1000	4097000
Total													**62,378,344**

Figure 7: AlexNet's layers and number of parameters

Chapter 4

GRAMIAN ANGULAR FIELD IMAGES

Gramian Angular Field is a time series encoding method. It was proposed by Zhiguang Wang and Tim Oates. GAF uses various operations to convert the time series data in the polar coordinate plane to the angular symmetry matrix. GASF or Gramian Angular Summation Field is a type of GAF.

Oates et al. proposed a framework for encoding time series as images, inspired by the recent achievements of deep learning in artificial intelligence [15].

In this study, three different methods are suggested. These methods are Gramian Angular Summation Field (GASF), Gramian Angular Difference Field (GADF), and Markov Transition Fields (MTF). These methods can be used in time series classifications and computer vision. Twenty standard datasets were used to test the three proposed methods. All data were tested on a CNN model. In order to determine the success rate of the proposed methods, they are compared with most of the best available time series classification methods. The results obtained are very promising. It is stated that it gives very good results compared to most existing methods.

Imaging Time Series

First, 2 separate frames are proposed to encode the time series as images. The first is a Gramian-Angular-Field (GASF) where time series are represented in a polar

coordinate system instead of Cartesian coordinates. In the Gramian matrix, each element corresponds to the cosine of the sum of the angles. In the second, Markov-Transition-Field (MTF) is proposed. The purpose of MTF is to construct the markov matrix after decomposition and encode the dynamic transition probability in the Gramian matrix.

Gramian Angular Field

First, all values of the time series are rescaled from 0 to 1 or from -1 to 1. The following formula was used for this process. Both formulas are used for scaling.

$$\tilde{x}^i_{-1} = \frac{(x_i - max(X) + (x_i - min(X))}{max(X) - min(X)}$$
$$\tilde{x}^i_0 = \frac{x_i - min(X)}{max(X) - min(X)}$$

Next, we can encode the 0 to 1 scale time series we get as the angular cosine and the timestamp as the radius. The following formula was used for this process.

$$\begin{cases} \phi = \arccos(\tilde{x_i}), -1 \leq \tilde{x_i} \leq 1, \tilde{x_i} \in \tilde{X} \\ r = \frac{t_i}{N}, t_i \in \mathbb{N} \end{cases}$$

The ti in this equation represents the timestamp. N is a constant value used for the polar coordinate system to improve the trajectory. This new polar-oriented system will be a new one for understanding time series. When the time value increasesi values are bent between different spaces in circles, like in a wave. There are two important features in this formula. cos(φ), φ ∈ [0, π]k is the monotonic bijective. Rescaled data has different angular boundaries. Gramian Angular Summation Field and Gramian Difference Field provide different levels of information granularity.The Gramian Angular Difference Field has the correct inverse map.

After converting the rescaled time series data to the polar coordinate system, we can easily take advantage of the angular perspective. Gramian-Angular-Summation-Field (GASF) and Gramian-Angular-Differential-Field (GADF) formulas are pictures.

$$\begin{aligned} GASF &= [\cos(\phi_i + \phi_j)] \\ &= \tilde{X}' \cdot \tilde{X} - \sqrt{I - \tilde{X}^2}' \cdot \sqrt{I - \tilde{X}^2} \end{aligned}$$

$$\begin{aligned} GADF &= [\sin(\phi_i - \phi_j)] \\ &= \sqrt{I - \tilde{X}^2}' \cdot \tilde{X} - \tilde{X}' \cdot \sqrt{I - \tilde{X}^2} \end{aligned}$$

GASF consists of 2 basic features. The first is to normalize the data in the range of 0 to 1. In other words, being able to transform GASF into normalized time series data using cross items. The second is to preserve absolute temporal relations with polar coordinates.

When converted to the polar coordinate system, the time series in each time step is taken as a one-dimensional metric space. GAFs have many advantages. As the position moves from top left to bottom right, they maintain temporal dependency. From the main diagonal, the time series can be reconstructed from high-level features learned by the deep neural network. GAFs are large relative to time series because they consist of nxn gramian matrices. It is possible to reduce this size.

The proposed method was compared with 9 different methods. For comparison, 20 different datasets were used. The results obtained are promising. It was stated that it gave very high results in 9 out of 20 datasets. Sufficiently high results were also obtained in the other 11 datasets.

Dataset	1NN-RAW	1NN-DTW-BWW	1NN-DTW-nWW	Fast-Shapelet	SAX-BoP	SAX-VSM	RPCD	SMTS	TSBF	GASF-GADF-MTF
50words •	0.369	0.242	0.31	N/A	0.466	N/A	0.2264	0.289	**0.209**	0.301 (16, 32)
Adiac ∗	0.389	0.391	0.396	0.514	0.432	0.381	0.3836	0.248	**0.245**	0.373 (32, 48)
Beef •	0.467	0.467	0.5	0.447	0.433	0.33	0.3667	0.26	0.287	**0.233 (64, 40)**
CBF †	0.148	0.004	0.003	0.053	0.013	0.02	N/A	0.02	**0.009**	**0.009 (32, 24)**
Coffee •	0.25	0.179	0.179	0.068	0.036	**0**	**0**	0.029	0.004	**0 (64, 48)**
ECG •	0.12	0.12	0.23	0.227	0.15	0.14	0.14	0.159	0.145	**0.09 (8, 32)**
FaceAll ∗	0.286	0.192	0.192	0.411	0.219	0.207	**0.1905**	0.191	0.234	0.237 (8, 48)
FaceFour ∗	0.216	0.114	0.17	0.090	0.023	**0**	0.0568	0.165	0.051	0.068 (8, 16)
fish ∗	0.217	0.16	0.167	0.197	0.074	**0.017**	0.1257	0.147	0.08	0.114 (8, 40)
Gun_Point ◁	0.087	0.087	0.093	0.061	0.027	0.007	**0**	0.011	0.011	0.08 (32, 32)
Lighting2 •	0.246	0.131	0.131	0.295	0.164	0.196	0.2459	0.269	0.257	**0.114 (16, 40)**
Lighting7 •	0.425	0.288	0.274	0.403	0.466	0.301	0.3562	**0.255**	0.262	0.260 (16, 48)
OliveOil •	0.133	0.167	0.133	0.213	0.133	0.1	0.1667	0.177	**0.09**	0.2 (8, 48)
OSULeaf ∗	0.483	0.384	0.409	0.359	0.256	**0.107**	0.3554	0.377	0.329	0.358 (16, 32)
SwedishLeaf ∗	0.213	0.157	0.21	0.269	0.198	0.01	0.0976	0.08	0.075	**0.065 (16, 48)**
synthetic control †	0.12	0.017	**0.007**	0.081	0.037	0.251	N/A	0.025	0.008	**0.007 (64, 48)**
Trace †	0.24	0.01	**0**	0.002	**0**	**0**	N/A	**0**	0.02	**0 (64, 48)**
Two Patterns †	0.09	0.0015	**0**	0.113	0.129	0.004	N/A	0.003	0.001	0.091 (64, 32)
wafer •	0.005	0.005	0.02	0.004	0.003	0.0006	0.0034	**0**	0.004	**0 (64, 16)**
yoga ∗	0.17	0.155	0.164	0.249	0.17	0.164	0.134	**0.094**	0.149	0.196 (8, 32)
#wins	0	0	3	0	1	5	3	4	4	**9**

Figure 8: GASF-GADF compared with 9 different methods

In conclusion, this article presents a set of formulas for converting to GASF, GADF and MTF images. A CNN model is used to test the performance of these methods. These methods, gave the most successful results in the application of many datasets compared to other methods. Using GASF, it has been shown to outperform raw data. It is foreseen that recurrent neural networks can be used in the future.

Chapter 5

K-FOLD CROSS VALIDATION

Cross-Validation is a statistical method that divides the data into many parts and enables train and test in different variations. [16] Each variation is compared and evaluated. In Cross-Validation, when creating train and test sets, each data segment is selected for training and testing in different variations. In this way, a crossover is made in successive rounds. The most basic of cross-validation is k-fold-cross-validation. In k-fold-cross-validation, the data is first segmented according to the given k value. For example, when k is selected as three, all data is split into three separate parts. Next, the first piece is reserved for testing and the other two pieces are used for the train. This is the first variation. In the second variation, the second piece is reserved for testing and the first and third pieces are used for training.

In the final variation, the third piece is reserved for testing and the first and second pieces are used for training. These 3 different variations are shown in the picture below. 3 separate boxes represent data. The light grey boxes represent the sections reserved for testing.

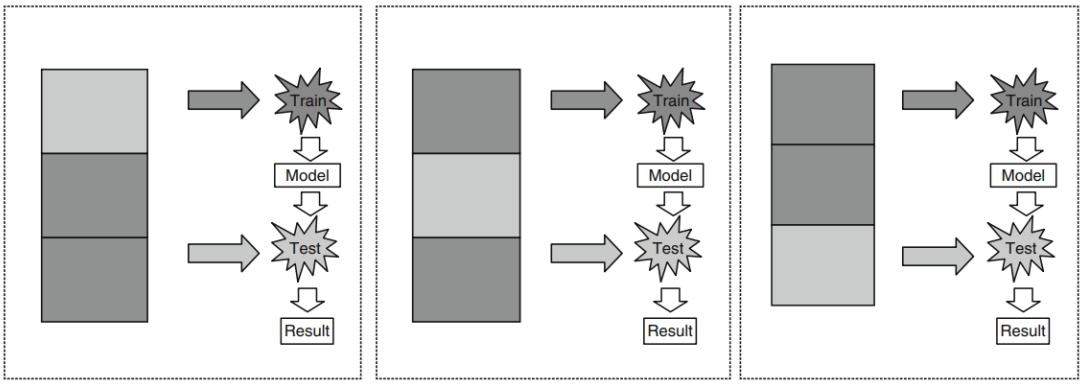

Figure 9: K-fold cross validation working logic [16]

In this way, not a single result, but a total of three results are obtained. Out of these three results using different variations, the one with the highest score is selected. In this way, it becomes possible to produce higher scores with different variations while training and testing, without relying on just one variation. The higher the K value is given, the higher the success rate will result. However, each time the value of k increases, the required processing load also increases. The main purpose of Cross-Validation is to evaluate and compare learning algorithms.

Chapter 6

METHODOLOGY

In this study, early diagnosis of Alzheimer's disease with EEG recordings. For this, it has been trained and tested in CNN architecture by converting EEG recordings to GASF images. There are many studies in the literature that provide early diagnosis of Alzheimer's disease with EEG recordings. The purpose of this study is to compare it with other studies by using GASF images. The reason for this is the high success rate of 2D images in CNN architecture. The success rate of CNN architecture in 2D images has been proven in the studies. For this reason, CNN was preferred as the artificial neural network.

In this study, early diagnosis of Alzheimer's disease was aimed using EEG data. In this study, F.J. Fraga, T.H. Falk, LR Trambaiolli, E.F. Oliveira, W.H.L. Pinaya, P.A.M. Kanda used the dataset collected by R. Anghinah [17][18][19]. The Matlab data files in the folder containing the EEG data of the subjects from the groups are NS, AD1, and AD2, respectively. Each .mat file contains 20-channel EEG periods of eight seconds recorded at a sampling rate of 200 Hz (1600 samples per period). The data is structured as a 3D matrix: 20 channels x 1600 samples x N periods. Channel tags (10-20 systems) are available in the channelNames.mat file. The file “ICASSP2013 PAPER (FRAGA) - SUBJECTS DEMOGRAPHIC DATA.xlsx” contains Gender, Age, MMSE, Education (years), and CDR information from all participants (sorted by group).

6.1 Participants

The data set consists of three parts. Healthy participants, Mild Alzheimer's patients and Alzheimer's patients. Healthy participants were designated NS. Mild Alzheimer's patients were named AD2 and Alzheimer's patients were named AD1. The data set consisted of 88 participants in total. Of these, 35 participants are healthy. 22 participants have mild Alzheimer's disease and 31 participants have Alzheimer's disease. Of the healthy participants, 16 were male and 19 were female. Of the Alzheimer's patients, 12 were male and 10 were female. Among the participants with mild Alzheimer's disease, 7 were male and 15 were female. The mean age of healthy participants was 66.89, the mean age of mild Alzheimer's patients was 73.77, and the mean age of participants with Alzheimer's disease was 75.23.

6.2 Data Collection

EEG data includes eight second periods of 20-channel EEG after 200 Hz output rate (1600 samples per period). Data is available as a 3D matrix: 20 channels x 1600 samples x N periods. Channels where EEG data are collected; C3, C4, Cz, F3, F4, F7, F8, FP1, FP2, Fz, O1, O2, Oz, P3, P4, Pz, T3, T4, T5 and T6.

6.3 Data Preprocessing

The data were processed using LetsWave6, LetsWave7 and EEGLAB functions in MATLAB environment. LetsWave custom scripts are used to monitor channels and signal lengths. Below are some of the images provided by the LetsWave7 plugin. Topography and headplot images of NS, AD1 and AD2 participants are given in the images below. In the pictures, the black dots represent the channels, and the colored parts represent the electrical activity in the brain. As seen in the bar graph next to the pictures, the blue colored areas represent regions in the brain where there is no

electrical activity. The red areas are the areas where the electrical activity is most intense.

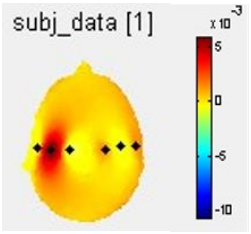

Figure 10: Headplot view with LetsWave7 AD1

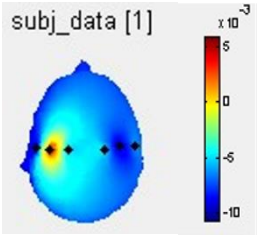

Figure 11: Headplot view with LetsWave7 AD2

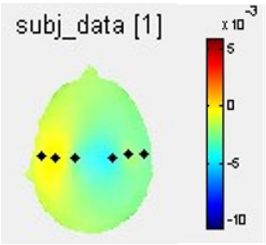

Figure 12: Headplot view with LetsWave7 NS

Each of the eeg records in the data set consists of records of at least 8 seconds. Records are not the same length. Below is the EEG recording of participant NS_003. In this image, all channels are listed under the heading channels. For example, the signal of the selected F7 channel is shown on the right side of the picture. Looking at the X-axis of the graph, it is seen that this record is collected in the range of approximately 0-87 seconds. Recordings were collected at 200 Hz. That's why there are 200 samples every second. There are 1600 samples in total in this sample record. On the Y axis of the graph, only the electrical activity of the F7 channel in the range of -7 - 10 is observed.

The record in Picture1 is filtered between 0 and 8. It started from 2 amplitude value when recording started and reached 1.5 amplitude value in the tenth digit. It then dropped to amplitude values of 2 at the seventh second. As seen in the graph, the electrical activity reached its highest level between 46-48 seconds with an amplitude value of 8.

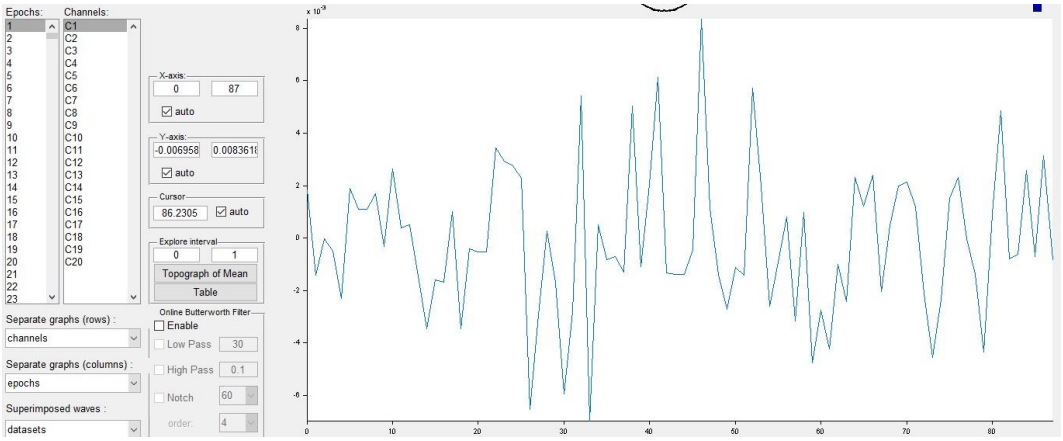

Figure 13: EEG recording of the NS_003 participant

When the filtering is narrowed and the range of 0-45 is examined, it is observed that the amplitude value is approximately 170. In figure 14, there is a filtered version of the range 0-45.

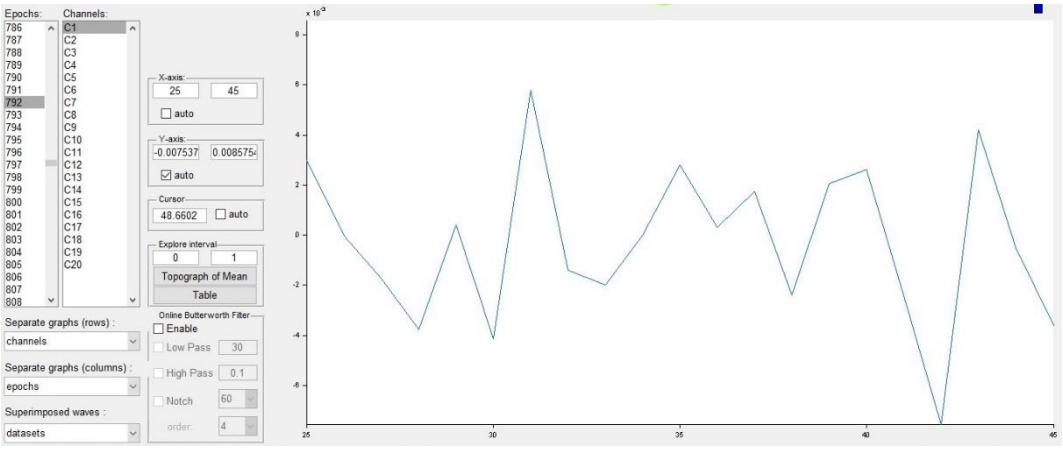

Figure 14: NS_003 filtered from 0-45 range of participant

LetsWave7 plugin does not allow us to export this data in csv format. Therefore, EEGLAB and MATLAB programs were used to export the data in csv format. The reason for using both LetsWave7 and EEGLAB is to analyze if data is corrupted during import. In order to analyze these differences that may occur in both programs, the F7 channel of the NS_003 participant was selected and compared. As seen in Figure 12 below, the F7 channel information of the NS_003 participant consists of a total of 1599 seconds. As seen in Letswave7, it consists of 1600 samples in total with 200Hz.

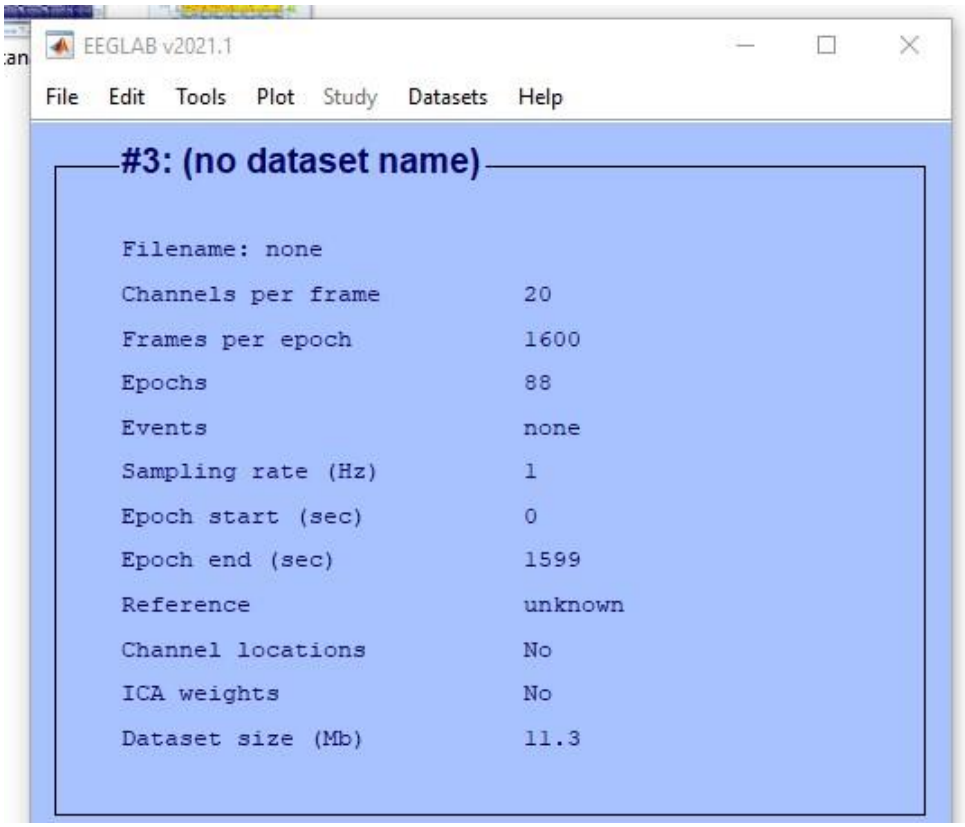

Figure 15: The O1 channel data of the NS_003 participant

When the 16 channels of the NS_003 participant are analyzed graphically using EEGLAB, the same results are observed with LetsWave7. According to these results, both programs gave the same results. Analysis can be done from both programs.

After checking the accuracy of the programs, the data on the F7 channel of the NS_003 participant was exported to be converted to csv format via the EEGLAB program. Then it was converted to csv format with matlab. The data to be converted to csv format was transferred to the matlab program.

All data were read in the generated matlab program so that the number of samples in each GASF image to be created would be 200 and it was converted into a csv file by the created program with 200 samples in each line. A csv file consisting of 12112 lines was created for each participant.

All of the mentioned transactions were made separately for each channel belonging to all participants. Then, csv files were created by combining all the data on a channel basis, including NS, AD1 and AD2.

CSV files were read separately by creating a program in CSV python language. Since there are negative and positive values for some channels in the values in the csv file read, first of all, all values are placed in the 0-1 range. Then, the values in the 0-1 range created were converted to GASF images.

A GASF image was generated for each 200 consecutive samples. The images were adjusted to be 128x128, taking into account the image sizes in similar studies. [20][21][22][23][24].

Three separate folders were created for each channel: NS, AD1 and AD2. Since there are 20 channels in total to be used in the train and test of the model, 20 separate folders

have been created. Channel names are given to these folders. Folders are made ready for training and testing.

All images that have been prepared are intended to be trained with a model. At this stage, it is desired to choose the most suitable neural network among many neural networks. Many articles have been reviewed on this subject.

Angelin Sarah et al. have presented a comprehensive article examining deep learning techniques related to EEG signal applications.[20] In this context, 156 articles on deep learning-based EEG applications between 2010 and 2018 were reviewed. This article provides an understanding of deep learning-based EEG applications and neural networks for various purposes. Many different network types and algorithms have been examined about deep learning. These; CNN, RNN, AE, RBM, MLPNN and DBN. In this article, It has been stated that Convolutional Neural Networks (CNN) are successful in processing nonlinear data. Also, It has been stated that convolutional neural networks give better results than recurrent neural networks in classifying EEG data. In the researches on CNN, accuracy, sensitivity and specificity rates of 15 different methods are presented. In these studies, 5-13 layered architectures were used. In addition, studies on RNN, AE, RBM and DBN and the results of these studies are presented. As a result, it was stated that convolutional neural networks, recurrent neural networks and deep belief networks performed better in EEG data. In particular, it has been stated that CNN and RNN have the highest performance rate in image recognition and nonlinear signals.

As a result of the researches, it has been understood that Convolutional Neural Networks are more successful than other neural networks in processing nonlinear data

and image recognition. For this reason, the Convolutional neural network model is used.

There are several terms that are commonly used along with the description of sensitivity, specificity and accuracy.

They are true positive (TP), true negative (TN), false negative (FN), and false positive (FP). If a disease is proven present in a patient, the given diagnostic test also indicates the presence of disease, the result of the diagnostic test is considered true positive. Similarly, if a disease is proven absent in a patient, the diagnostic test suggests the disease is absent as well, the test result is true negative (TN). Both true positive and true negative suggest a consistent result between the diagnostic test and the proven condition (also called standard of truth). However, no medical test is perfect. If the diagnostic test indicates the presence of disease in a patient who actually has no such disease, the test result is false positive (FP). Similarly, if the result of the diagnosis test suggests that the disease is absent for a patient with disease for sure, the test result is false negative (FN). Both false positive and false negative indicate that the test results are opposite to the actual condition.

Sensitivity, specificity and accuracy are described in terms of TP, TN, FN and FP.

Sensitivity = TP/(TP + FN) = (Number of true positive assessment)/(Number of all positive assessment)

Specificity = TN/(TN + FP) = (Number of true negative assessment)/(Number of all negative assessment)

Accuracy = (TN + TP)/(TN+TP+FN+FP) = (Number of correct assessments)/Number of all assessments

Chapter 7

RESULTS AND DISCUSSIONS

7.1 Preparation of the Working Environment

The NS, AD1 and AD2 folders were created by combining the data from all channels. The AlexNet model was created to perform training and testing operations. With these images it is desired to train and test operations on several personal computers using the AlexNet model. These images were attempted to be processed by the CPU on personal computers. However, due to the slow and insufficient processing power of the CPU in image processing, it was not possible to train and test all the data. In further research, the GPU was found to be faster in image processing [25][26][27]. GPU-Tensorflow, GPU-Keras, CUDNN and CudaToolkit have been installed on personal computers so that these operations can be performed through the GPU. However, due to the insufficient memory capacity of GPUs in personal computers, it was not possible to work with GPUs. Therefore, the search for a virtual machine began and the pro version of Google Colab, owned by Google, was rented. Google Colap pro version provides GPU, TPU and high memory usage. All images are uploaded to Google Drive so they can be read through Google Colab pro. Two separate issues were encountered while trying to train and test using all images in Google Colab. First, the request to read the images times out because there are a lot of images. Another problem is that Google Cloab's GPU and memory capacity is insufficient for all images. There is only one possibility left. It is training and testing by selecting only some channels, not all channels. A few studies have been reviewed on this topic. In these studies it was

understood that these processes were carried out by selecting 3 or 4 channels. Channel selection is randomly selected on some items. However, in some studies, all the channels were trained and tested one by one, and the channels with the highest results were selected. These 16 channels have been selected. After that, all the channels were individually trained and tested to observe the results of all the selected channels. The list of these 16 selected channels are: C3, C4, F3, F4, F7, F8, FP1, FP2, O1, O2, P3, P4, T3, T4, T5 and T6. The selected channels are shown in figure 16.

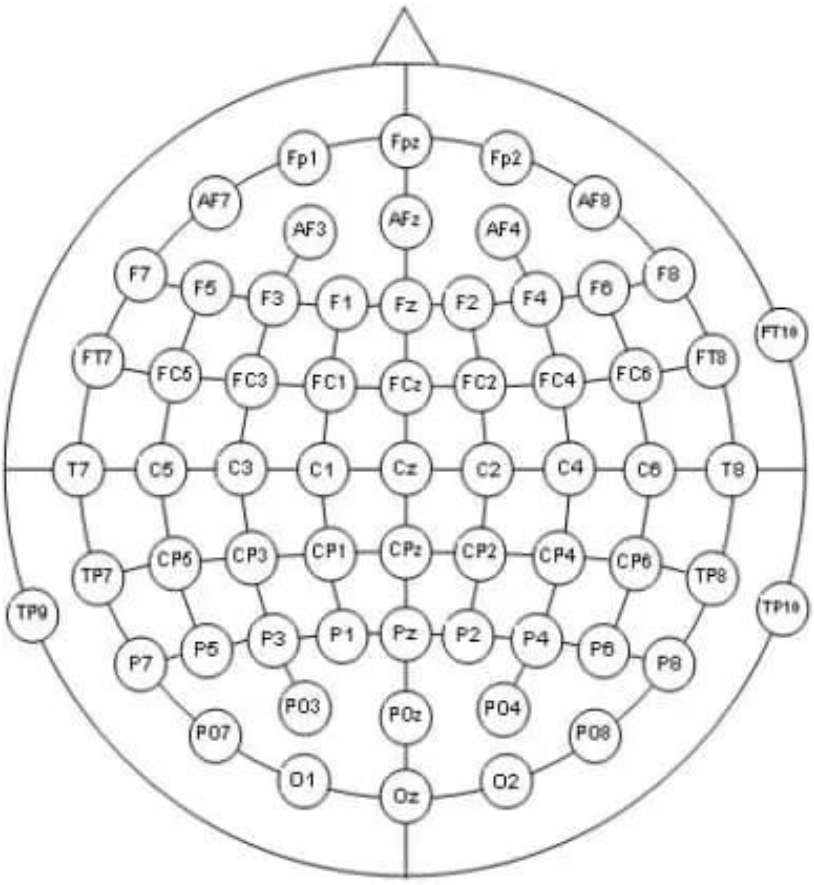

Figure 16: Selected channels for train and test

Below are the results obtained for all selected channels.

7.1.1 EEG Channel F7

The data of the F7 channel is divided into AD1 and NS. Then, these data were trained and tested with AlexNet deep learning model using Google Colap. Obtained results are presented below.

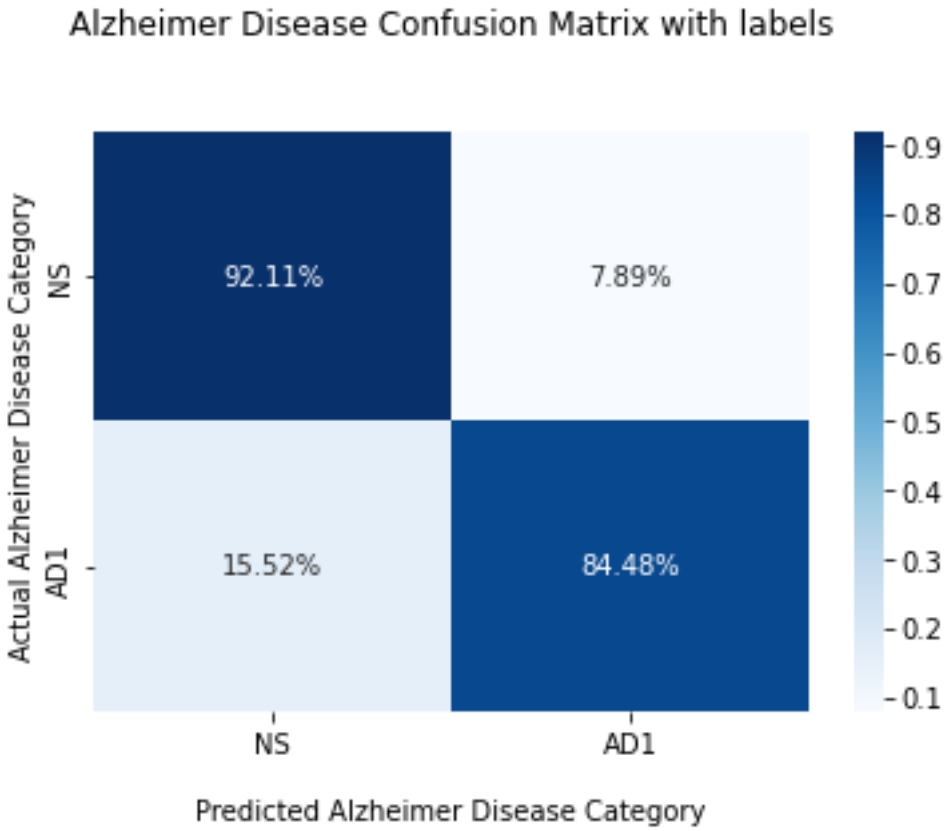

Figure 17: F7 channel NS and AD1 Confusion Matrix

Accuracy = 0. 8880597014925373

Sensitivity = 0. 8448275862068966

Specificity = 0. 9210526315789473

The data of the F7 channel is divided into AD2 and NS. Then, these data were trained and tested with AlexNet deep learning model using Google Colap. Obtained results are presented below.

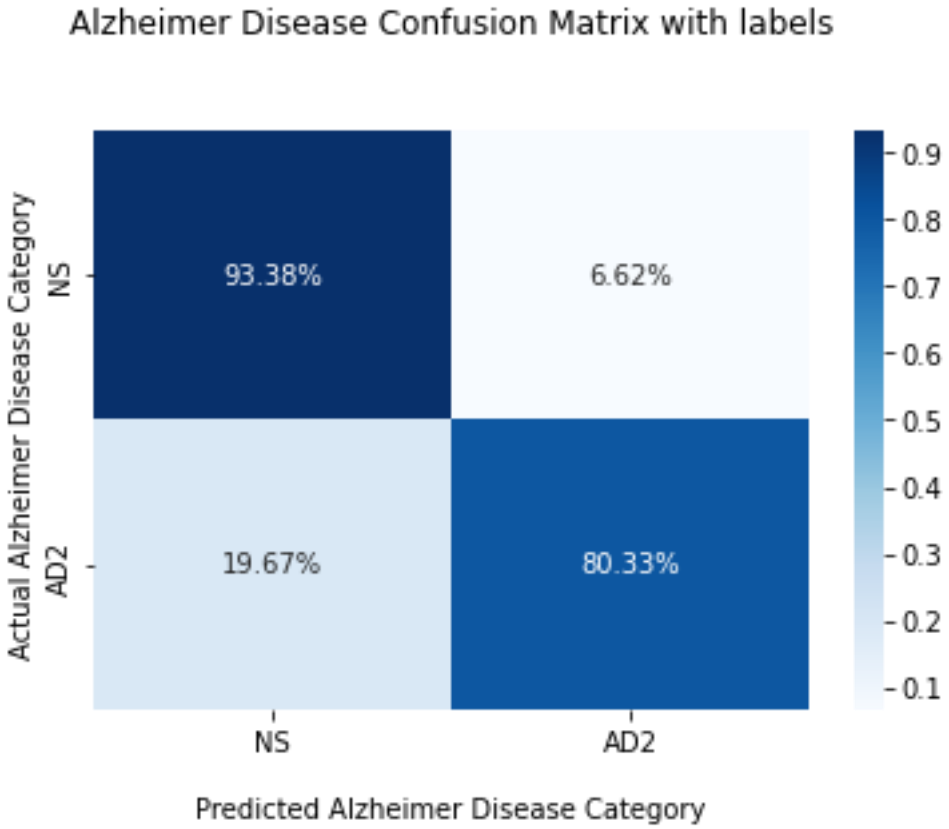

Figure 18: F7 channel NS and AD2 Confusion Matrix

Accuracy = 0. 872093023255814

Sensitivity = 0. 8032786885245902

Specificity = 0. 9338235294117647

7.1.2 EEG Channel T3

The data of the T3 channel is divided into AD1 and NS. Then, these data were trained and tested with AlexNet deep learning model using Google Colap. Obtained results are presented below.

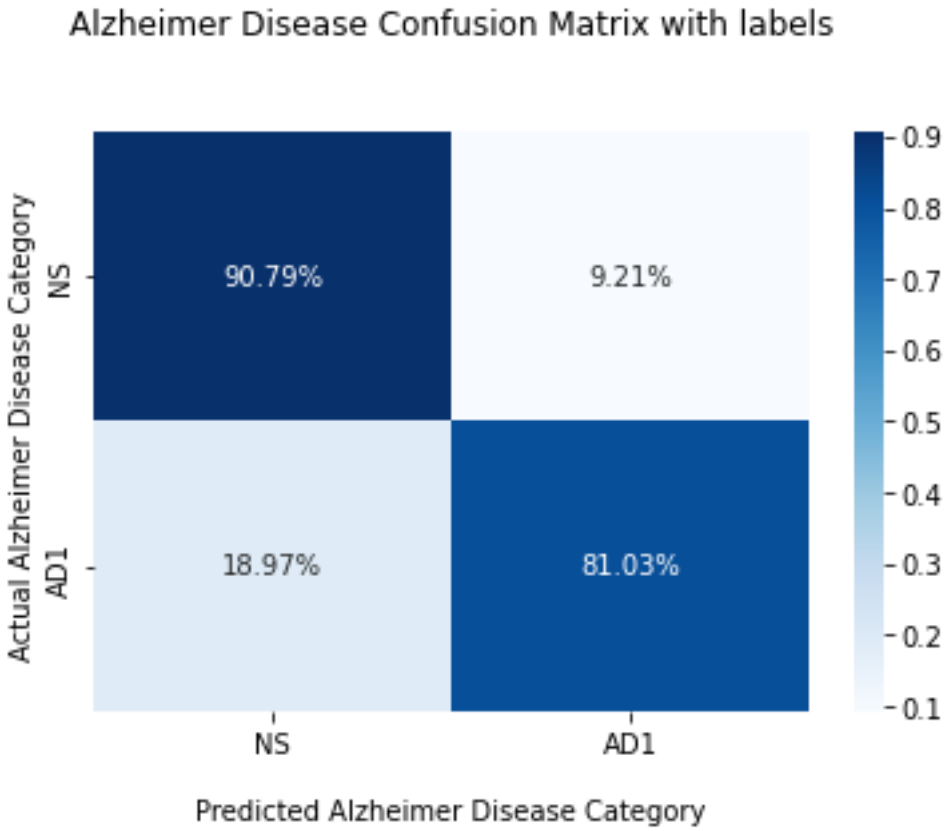

Figure 19: T3 channel NS and AD1 Confusion Matrix

Accuracy = 0. 8656716417910447

Sensitivity = 0. 8103448275862069

Specificity = 0. 9078947368421053

The data of the T3 channel is divided into AD2 and NS. Then, these data were trained and tested with AlexNet deep learning model using Google Colap. Obtained results are presented below.

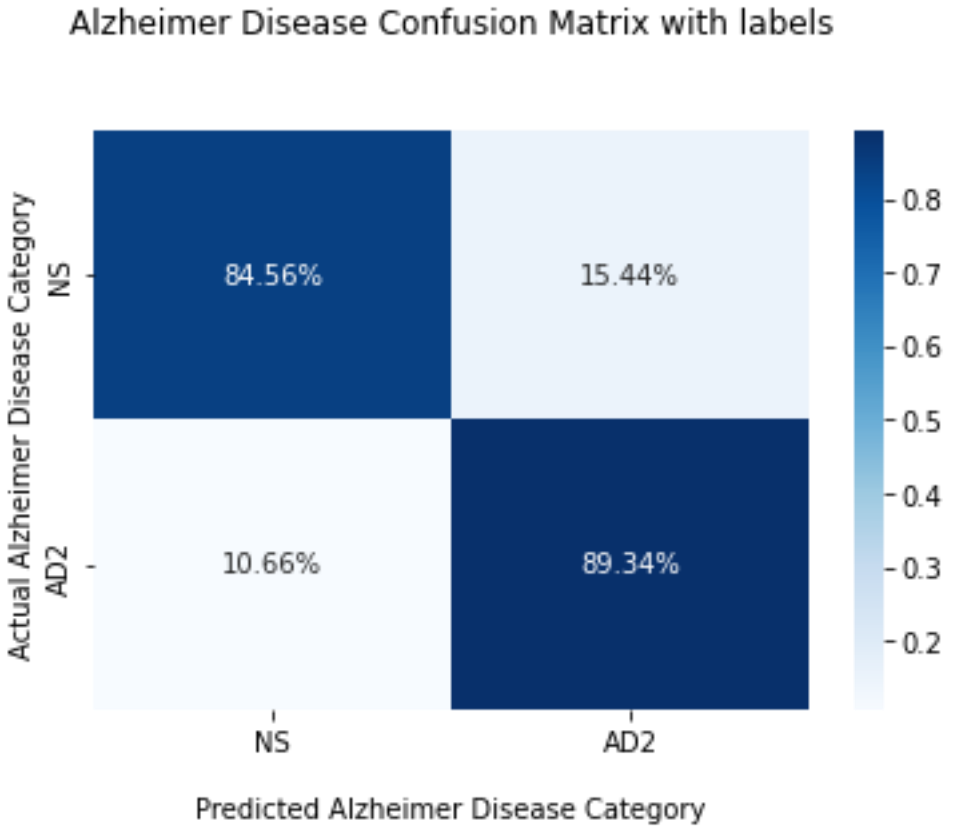

Figure 20: T3 channel NS and AD2 Confusion Matrix

Accuracy = 0. 8682170542635659

Sensitivity = 0. 8934426229508197

Specificity = 0. 8455882352941176

7.1.3 EEG Channel T5

The data of the T5 channel is divided into AD1 and NS. Then, these data were trained and tested with AlexNet deep learning model using Google Colap. Obtained results are presented below.

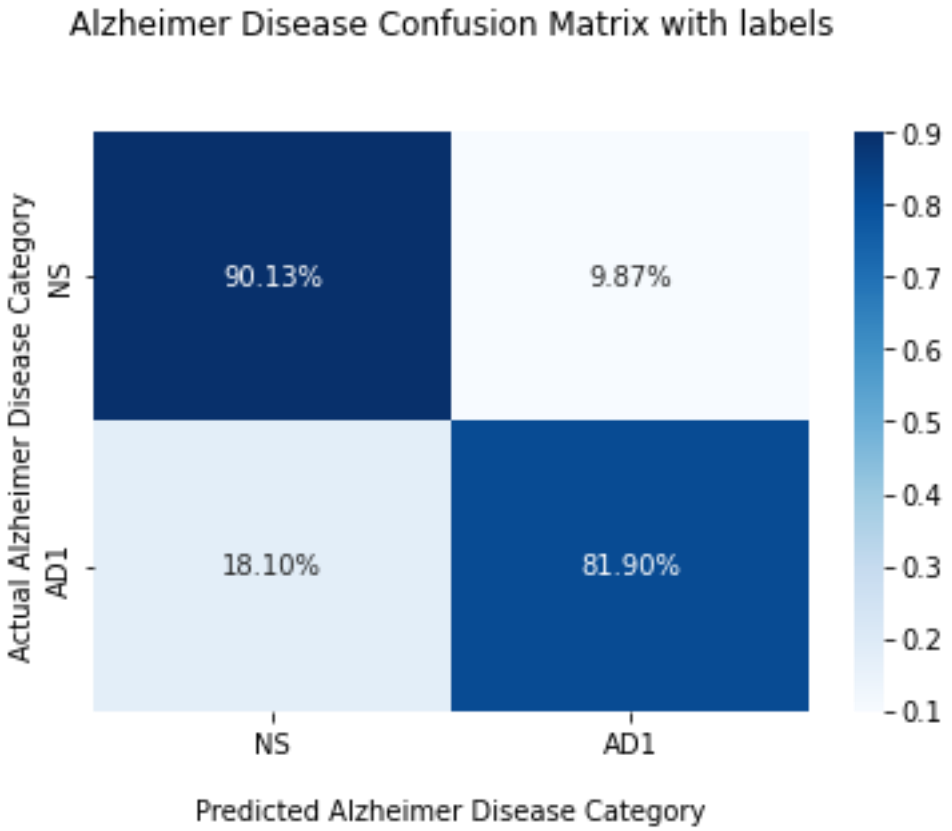

Figure 21: T5 channel NS and AD1 Confusion Matrix

Accuracy = 0. 8656716417910447

Sensitivity = 0. 8189655172413793

Specificity = 0. 9013157894736842

The data of the T5 channel is divided into AD2 and NS. Then, these data were trained and tested with AlexNet deep learning model using Google Colap. Obtained results are presented below.

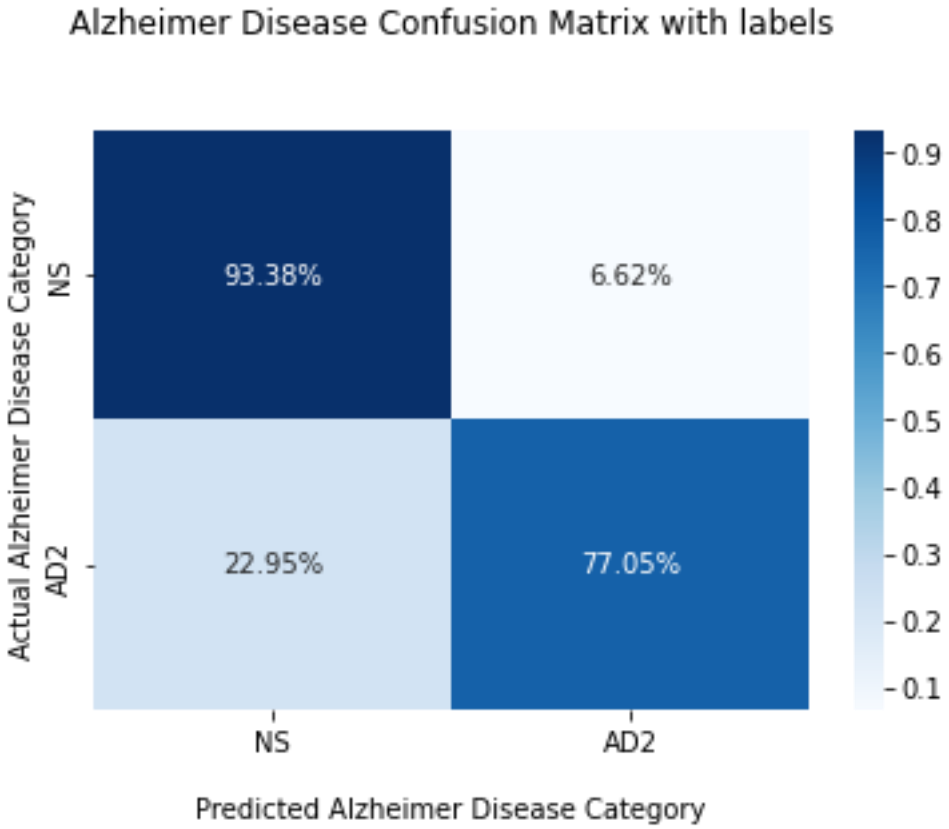

Figure 22: T5 channel NS and AD2 Confusion Matrix

Accuracy = 0. 8565891472868217

Sensitivity = 0. 7704918032786885

Specificity = 0. 9338235294117647

7.1.4 EEG Channel Fp1

The data of the Fp1 channel is divided into AD1 and NS. Then, these data were trained and tested with AlexNet deep learning model using Google Colap. Obtained results are presented below.

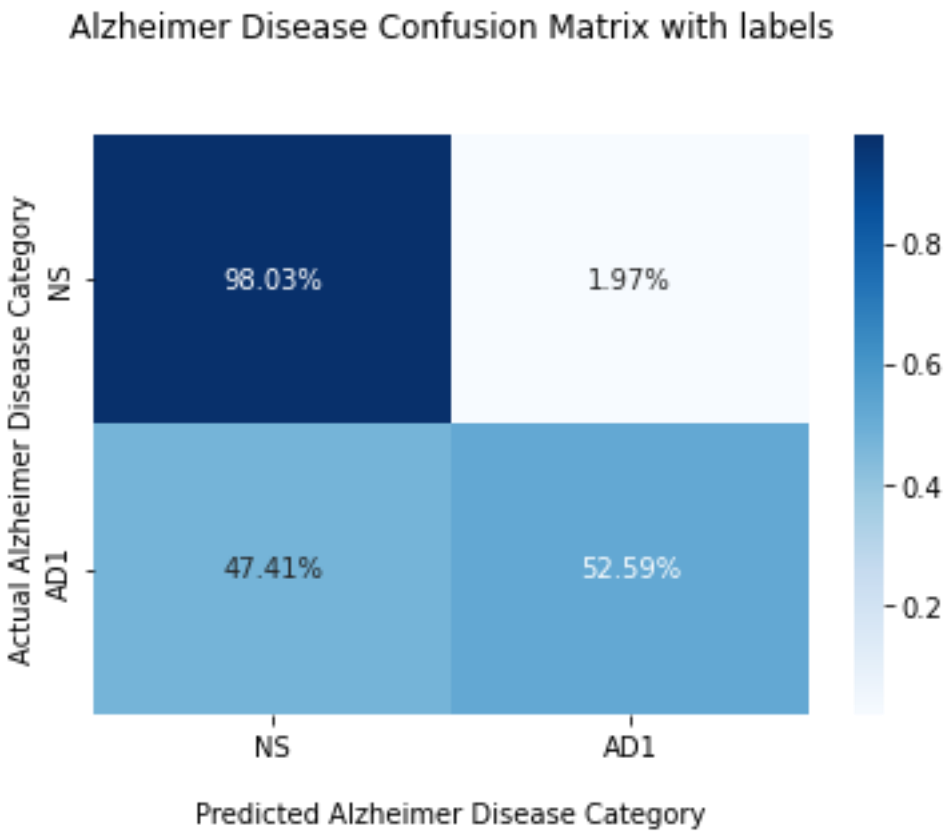

Figure 23: Fp1 channel NS and AD1 Confusion Matrix

Accuracy = 0. 7835820895522388

Sensitivity = 0. 5258620689655172

Specificity = 0. 9802631578947368

The data of the Fp1 channel is divided into AD2 and NS. Then, these data were trained and tested with AlexNet deep learning model using Google Colap. Obtained results are presented below.

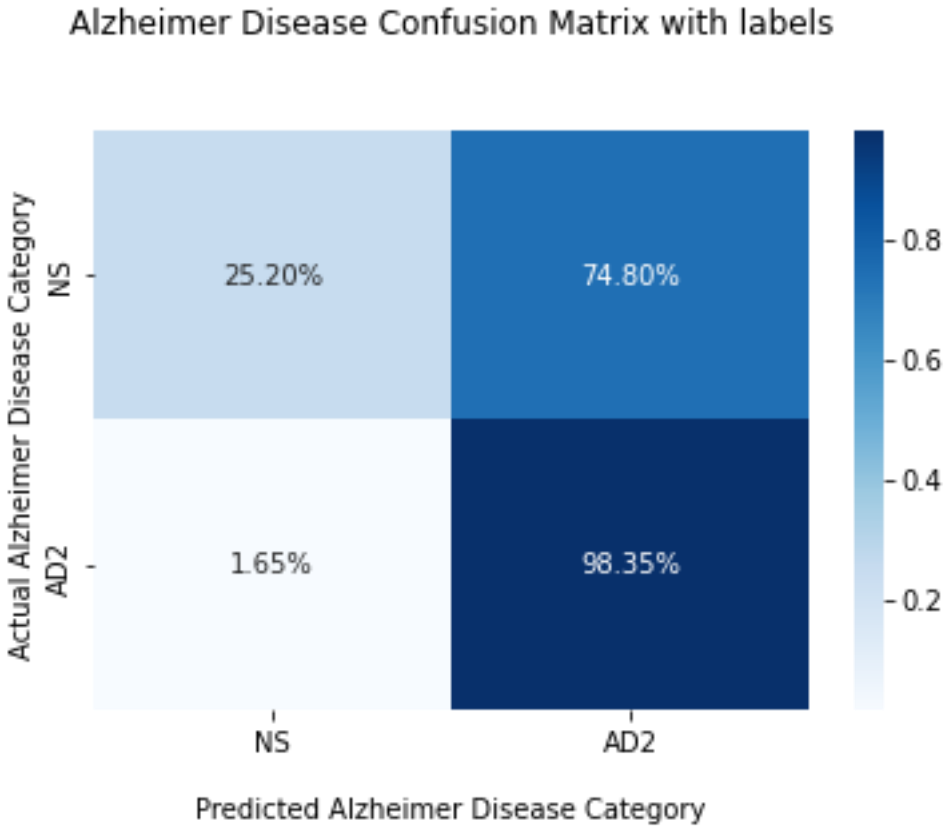

Figure 24: Fp1 channel NS and AD2 Confusion Matrix

Accuracy = 0. 6088709677419355

Sensitivity = 0. 9834710743801653

Specificity = 0. 25196850393700787

7.1.5 EEG Channel F3

The data of the F3 channel is divided into AD1 and NS. Then, these data were trained and tested with AlexNet deep learning model using Google Colap. Obtained results are presented below.

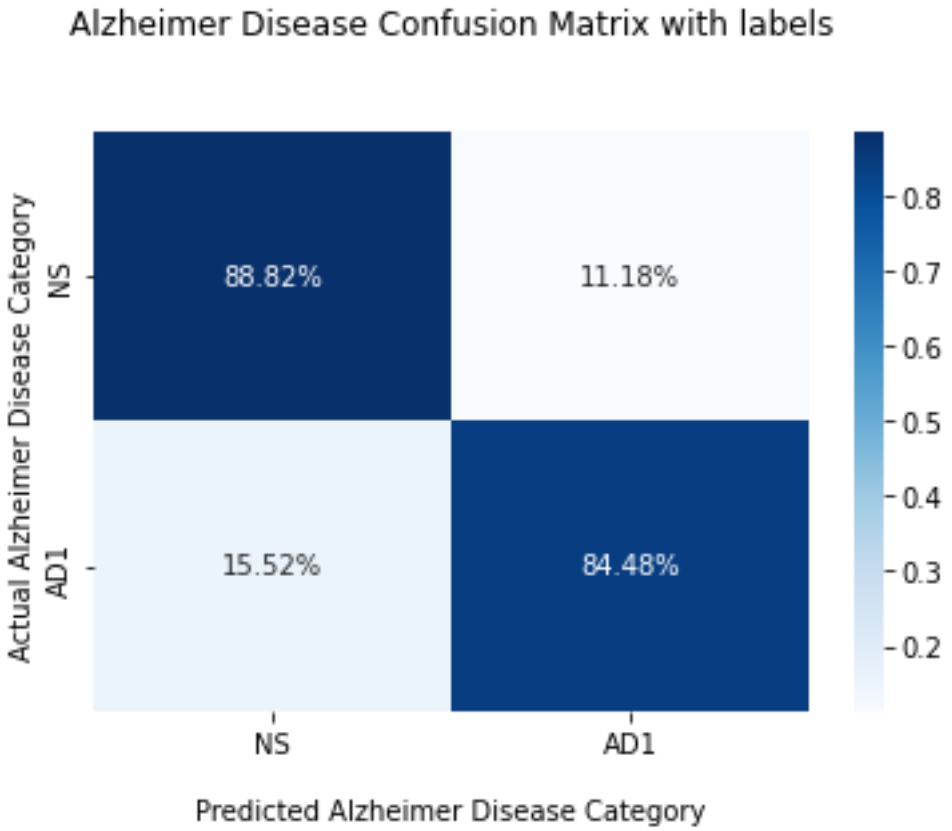

Figure 25: F3 channel NS and AD1 Confusion Matrix

Accuracy = 0. 8694029850746269

Sensitivity = 0. 8448275862068966

Specificity = 0. 8881578947368421

The data of the F3 channel is divided into AD2 and NS. Then, these data were trained and tested with AlexNet deep learning model using Google Colap. Obtained results are presented below.

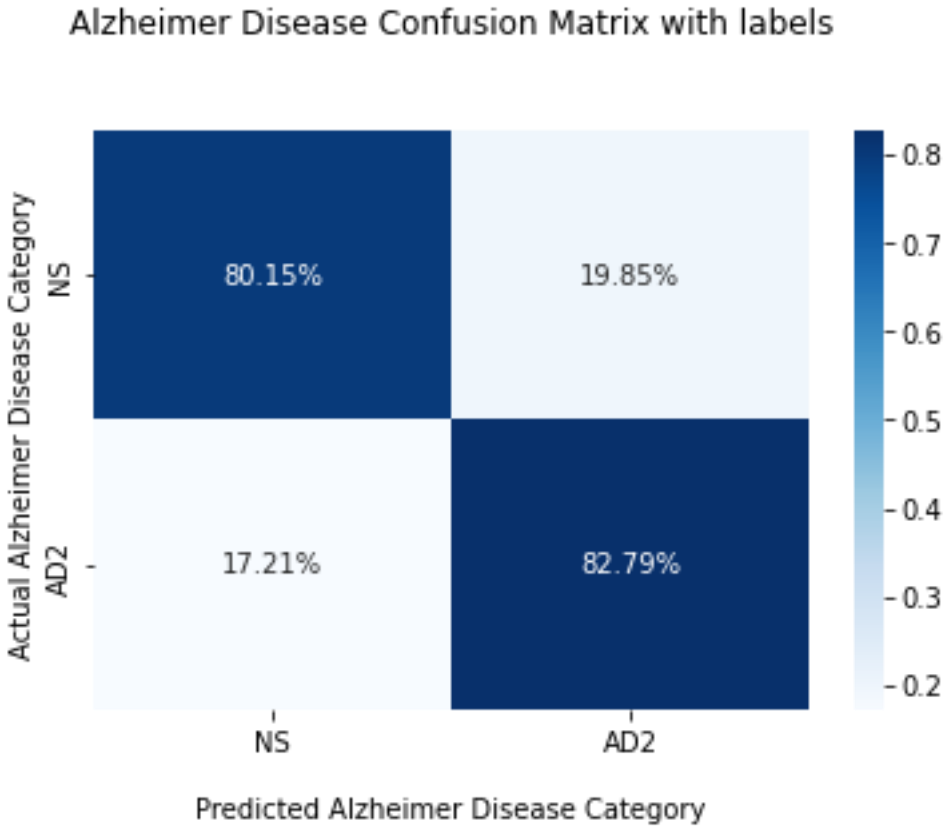

Figure 26: F3 channel NS and AD2 Confusion Matrix

Accuracy = 0. 813953488372093

Sensitivity = 0. 8278688524590164

Specificity = 0. 8014705882352942

7.1.6 EEG Channel C3

The data of the C3 channel is divided into AD1 and NS. Then, these data were trained and tested with AlexNet deep learning model using Google Colap. Obtained results are presented below.

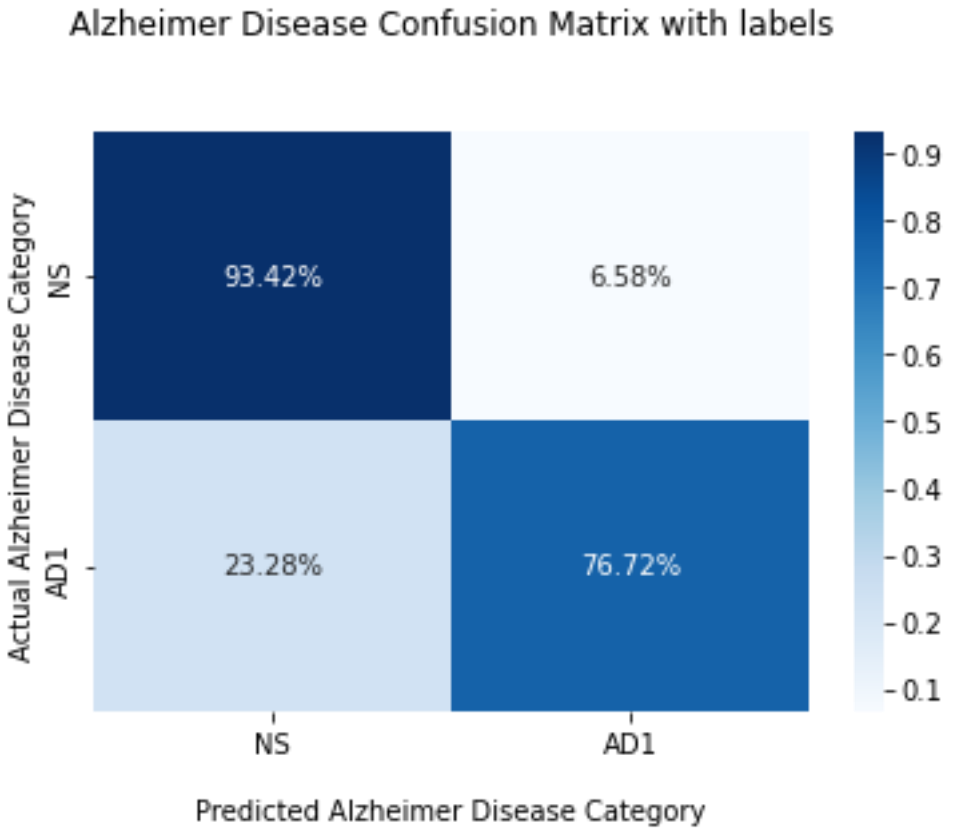

Figure 27: C3 channel NS and AD1 Confusion Matrix

Accuracy = 0. 8619402985074627

Sensitivity = 0. 7672413793103449

Specificity = 0. 9342105263157895

The data of the C3 channel is divided into AD2 and NS. Then, these data were trained and tested with AlexNet deep learning model using Google Colap. Obtained results are presented below.

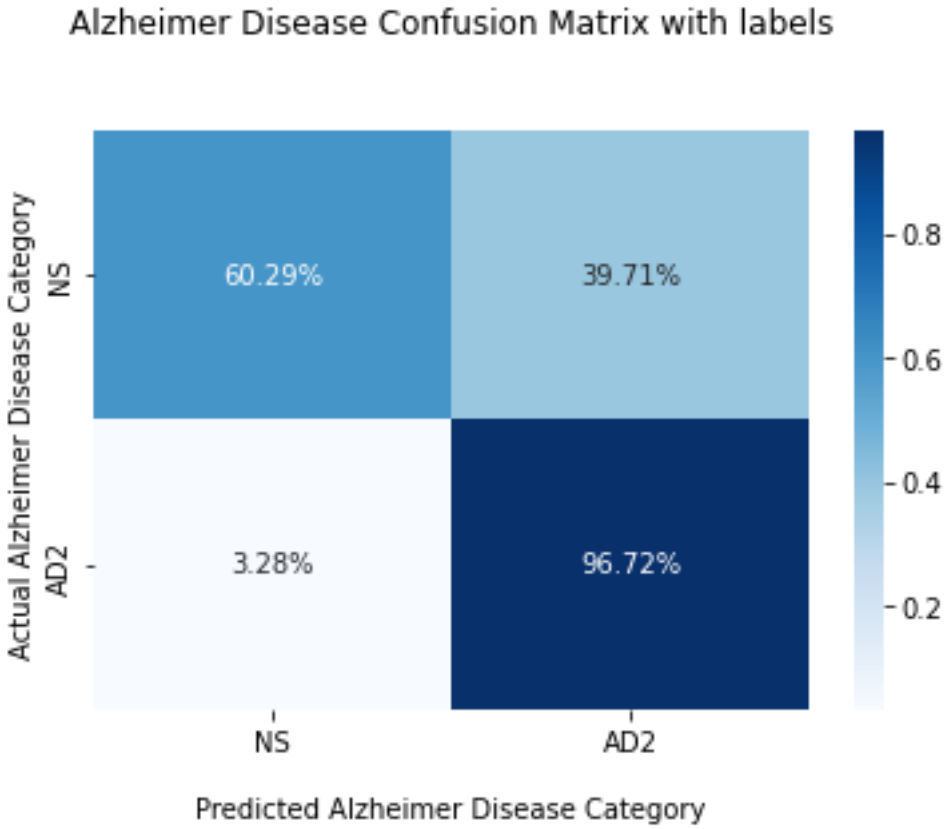

Figure 28: C3 channel NS and AD2 Confusion Matrix

Accuracy = 0. 7751937984496124

Sensitivity = 0. 9672131147540983

Specificity = 0. 6029411764705882

7.1.7 EEG Channel P3

The data of the P3 channel is divided into AD1 and NS. Then, these data were trained and tested with AlexNet deep learning model using Google Colap. Obtained results are presented below.

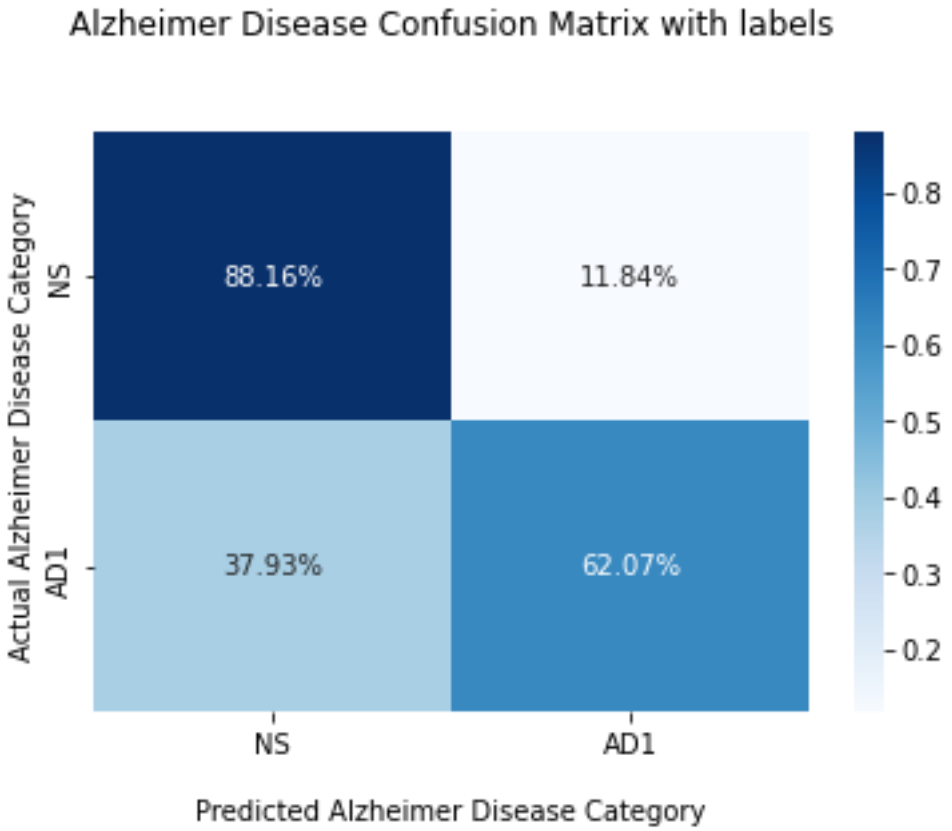

Figure 29: P3 channel NS and AD1 Confusion Matrix

Accuracy = 0. 7686567164179104

Sensitivity = 0. 6206896551724138

Specificity = 0. 881578947368421

The data of the P3 channel is divided into AD2 and NS. Then, these data were trained and tested with AlexNet deep learning model using Google Colap. Obtained results are presented below.

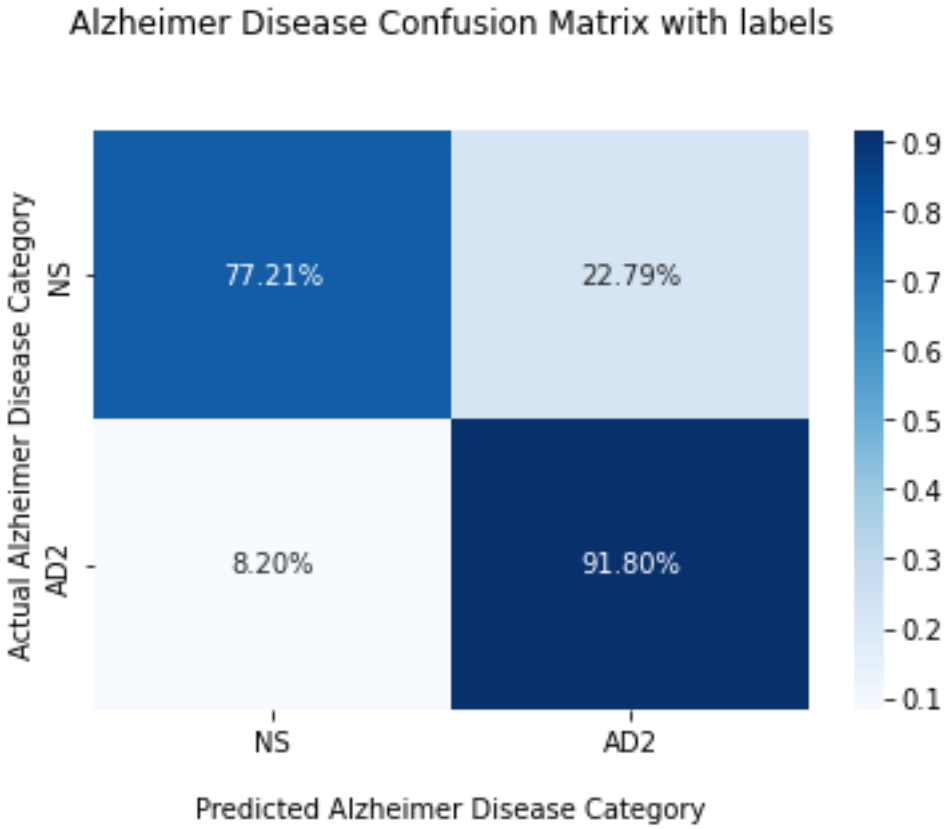

Figure 30: P3 channel NS and AD2 Confusion Matrix

Accuracy = 0. 8410852713178295

Sensitivity = 0. 9180327868852459

Specificity = 0. 7720588235294118

7.1.8 EEG Channel O1

The data of the O1 channel is divided into AD1 and NS. Then, these data were trained and tested with AlexNet deep learning model using Google Colap. Obtained results are presented below.

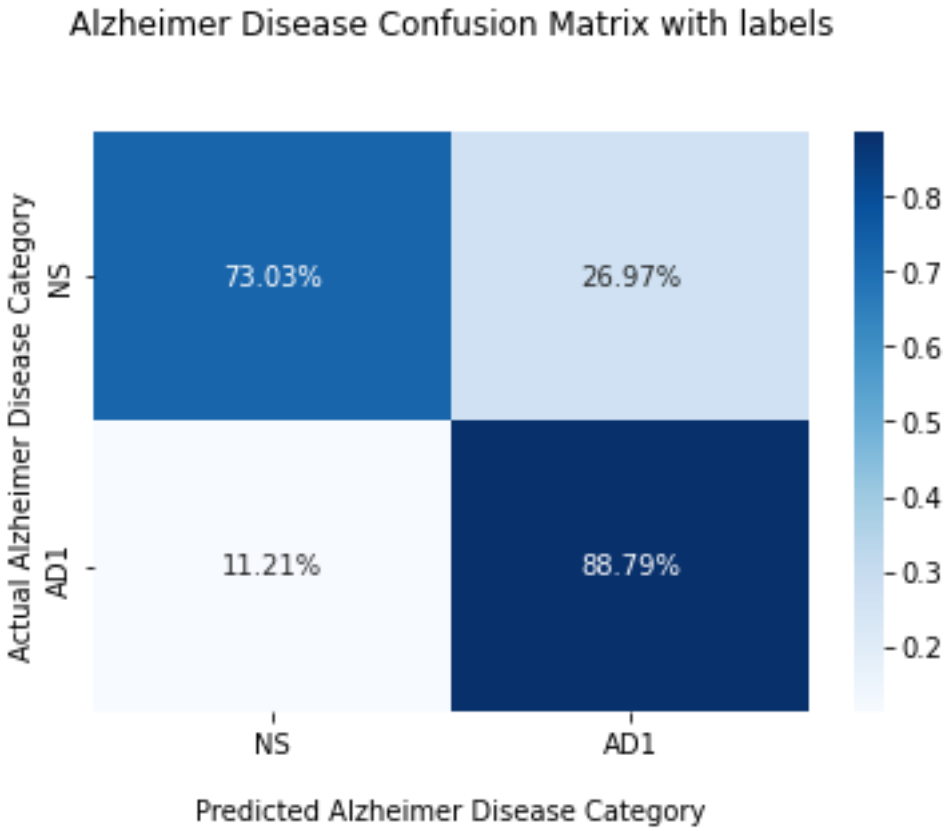

Figure 31: O1 channel NS and AD1 Confusion Matrix

Accuracy = 0. 7985074626865671

Sensitivity = 0. 8879310344827587

Specificity = 0. 7302631578947368

The data of the O1 channel is divided into AD2 and NS. Then, these data were trained and tested with AlexNet deep learning model using Google Colap. Obtained results are presented below.

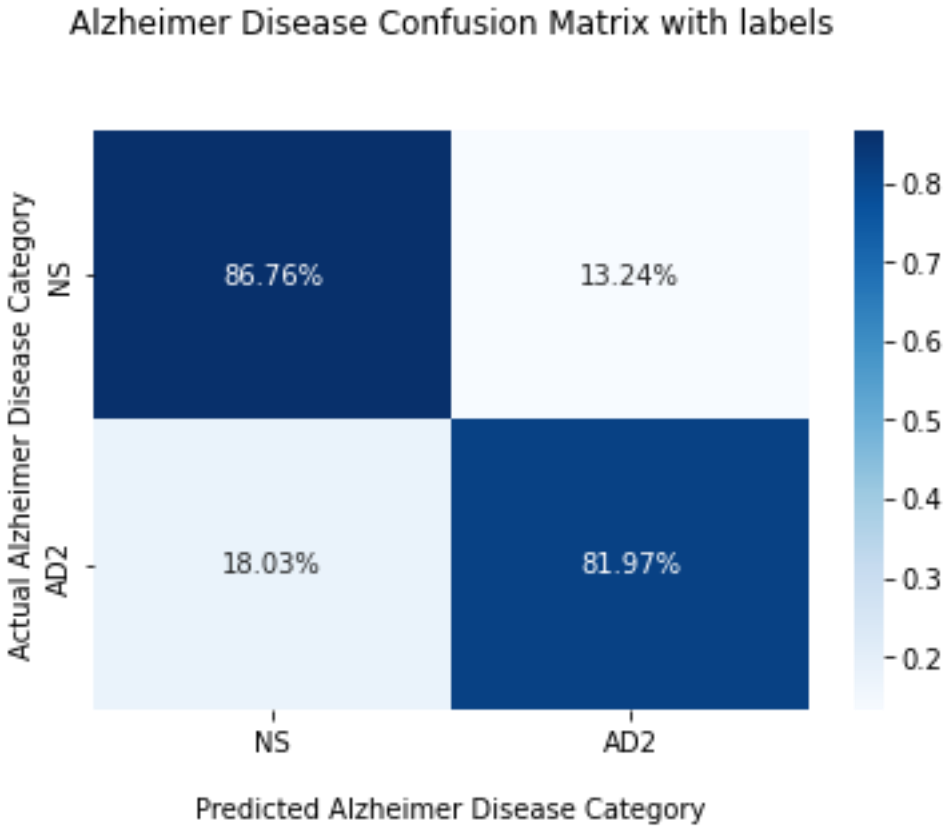

Figure 32: O1 channel NS and AD2 Confusion Matrix

Accuracy = 0. 8449612403100775

Sensitivity = 0. 819672131147541

Specificity = 0. 8676470588235294

7.1.9 EEG Channel F8

The data of the F8 channel is divided into AD1 and NS. Then, these data were trained and tested with AlexNet deep learning model using Google Colap. Obtained results are presented below.

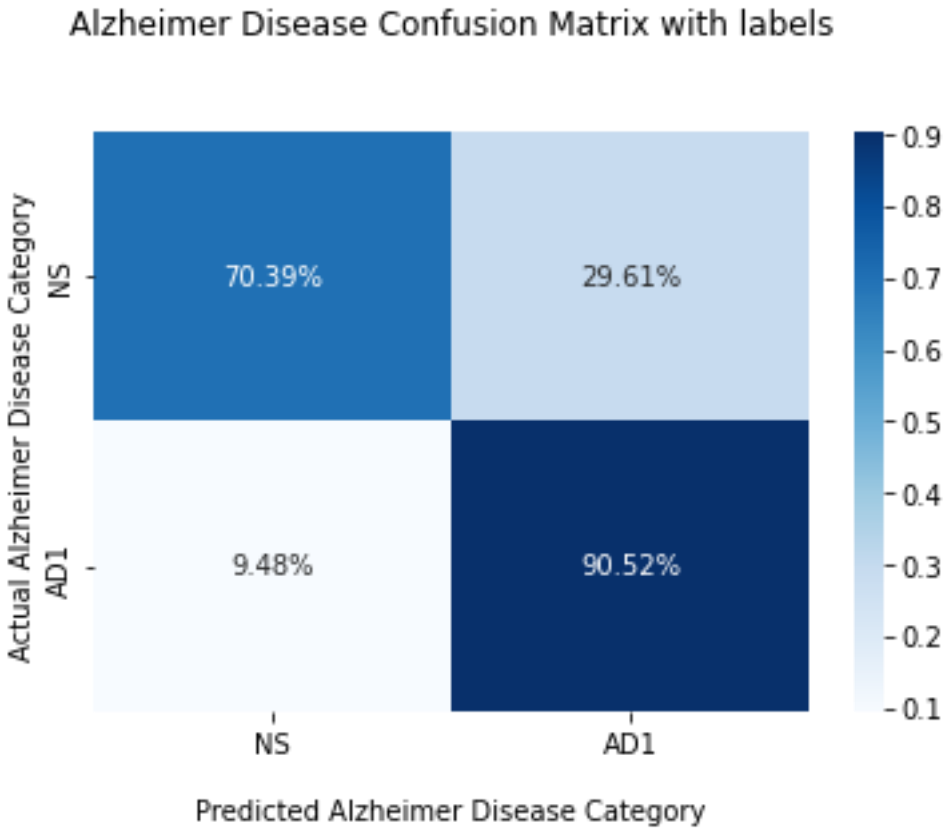

Figure 33: F8 channel NS and AD1 Confusion Matrix

Accuracy = 0. 7910447761194029

Sensitivity = 0. 9051724137931034

Specificity = 0. 7039473684210527

The data of the F8 channel is divided into AD2 and NS. Then, these data were trained and tested with AlexNet deep learning model using Google Colap. Obtained results are presented below.

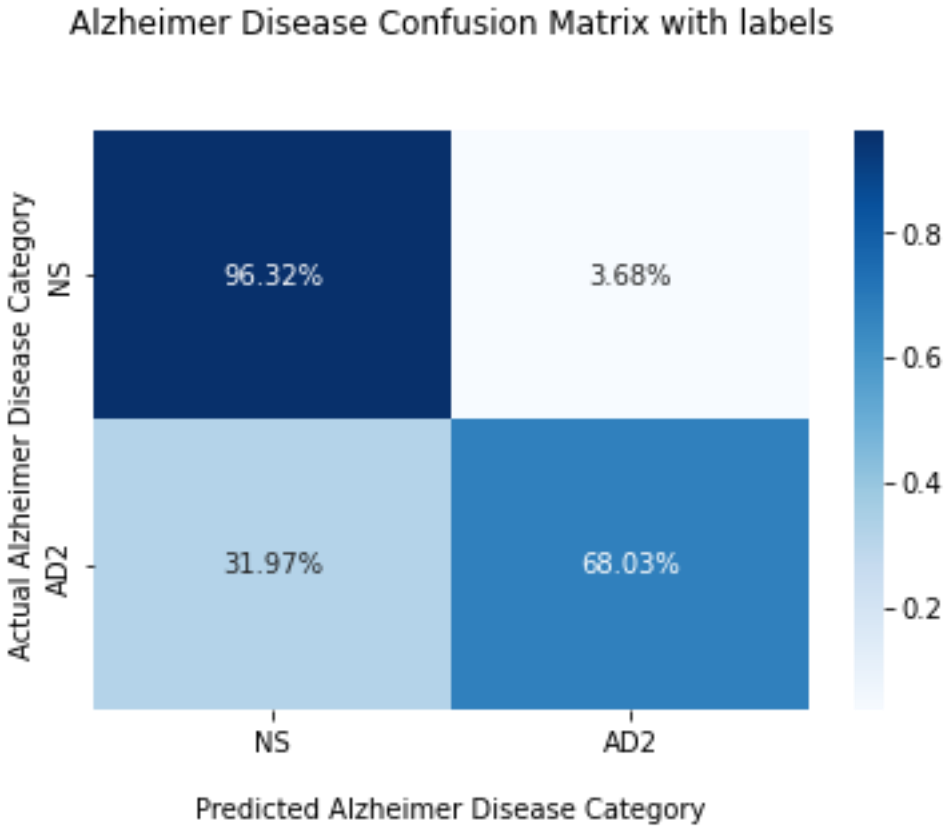

Figure 34: F8 channel NS and AD2 Confusion Matrix

Accuracy = 0. 8294573643410853

Sensitivity = 0. 680327868852459

Specificity = 0. 9632352941176471

7.1.10 EEG Channel T4

The data of the T4 channel is divided into AD1 and NS. Then, these data were trained and tested with AlexNet deep learning model using Google Colap. Obtained results are presented below.

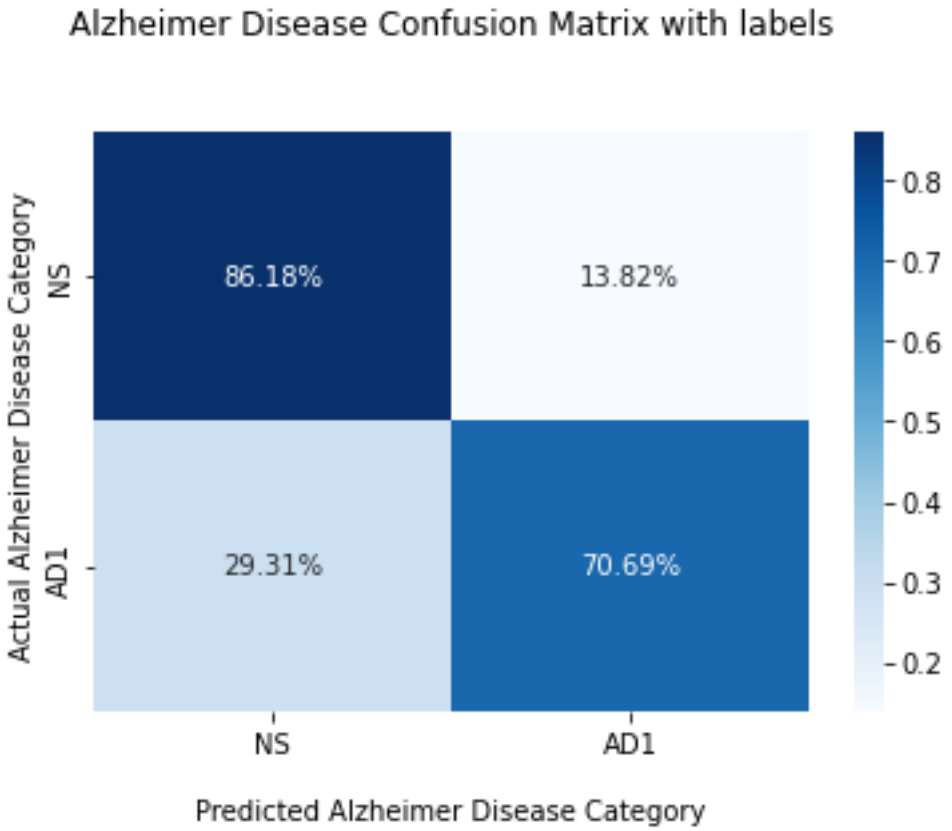

Figure 35: T4 channel NS and AD1 Confusion Matrix

Accuracy = 0. 7947761194029851

Sensitivity = 0. 7068965517241379

Specificity = 0. 8618421052631579

The data of the T4 channel is divided into AD2 and NS. Then, these data were trained and tested with AlexNet deep learning model using Google Colap. Obtained results are presented below.

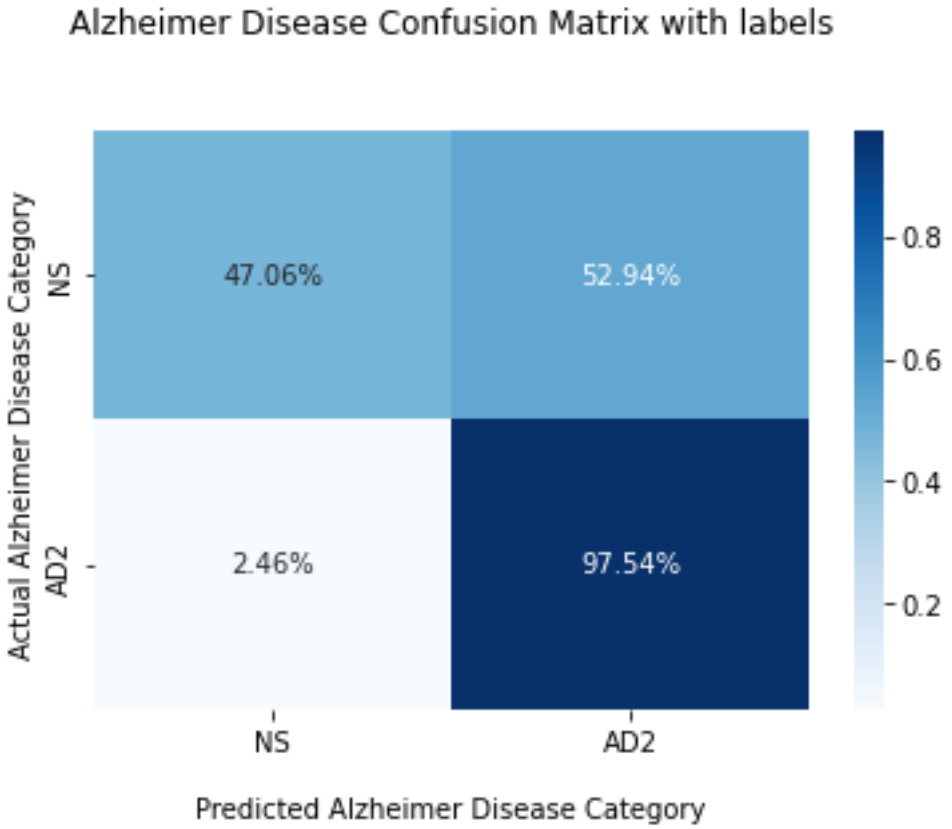

Figure 36: T4 channel NS and AD2 Confusion Matrix

Accuracy = 0. 7093023255813954

Sensitivity = 0. 9754098360655737

Specificity = 0. 47058823529411764

7.1.11 EEG Channel T6

The data of the T6 channel is divided into AD1 and NS. Then, these data were trained and tested with AlexNet deep learning model using Google Colap. Obtained results are presented below.

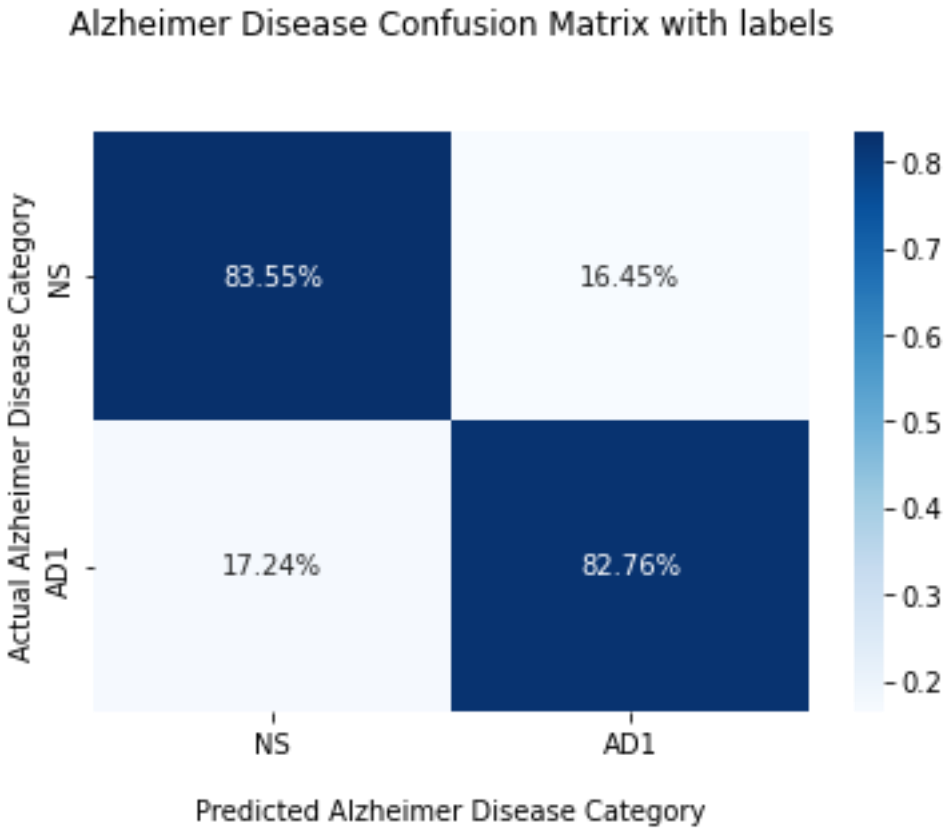

Figure 37: T6 channel NS and AD1 Confusion Matrix

Accuracy = 0. 832089552238806

Sensitivity = 0. 8275862068965517

Specificity = 0. 8355263157894737

The data of the T6 channel is divided into AD2 and NS. Then, these data were trained and tested with AlexNet deep learning model using Google Colap. Obtained results are presented below.

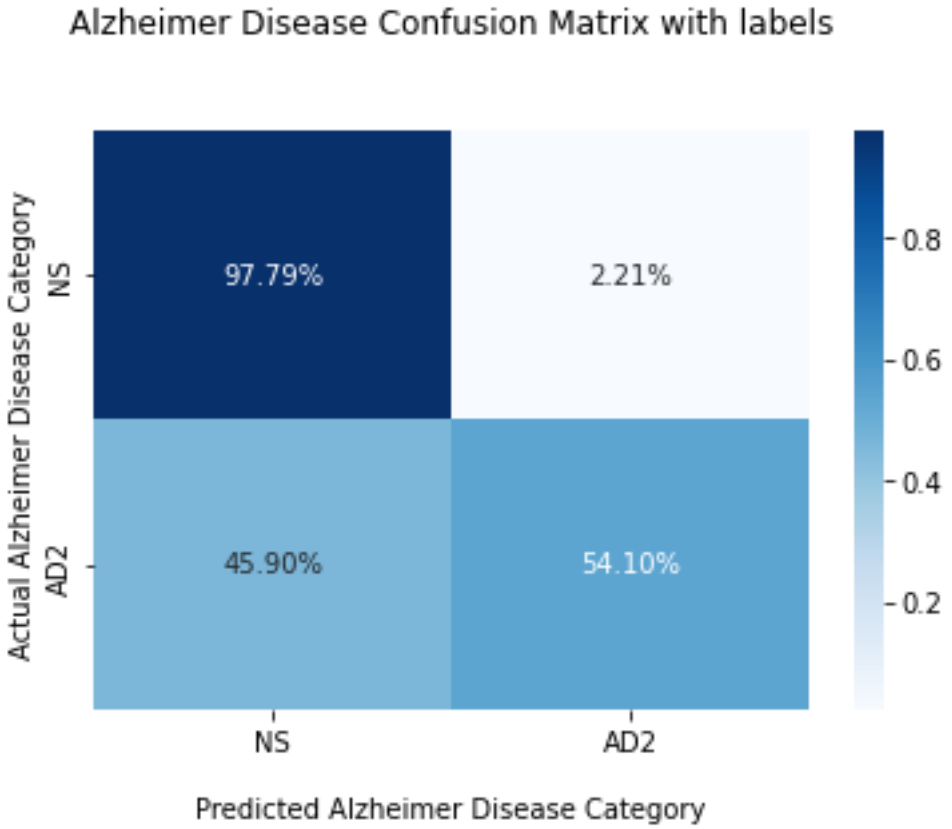

Figure 38: T6 channel NS and AD2 Confusion Matrix

Accuracy = 0. 7713178294573644

Sensitivity = 0. 5409836065573771

Specificity = 0. 9779411764705882

7.1.12 EEG Channel Fp2

The data of the Fp2 channel is divided into AD1 and NS. Then, these data were trained and tested with AlexNet deep learning model using Google Colap. Obtained results are presented below.

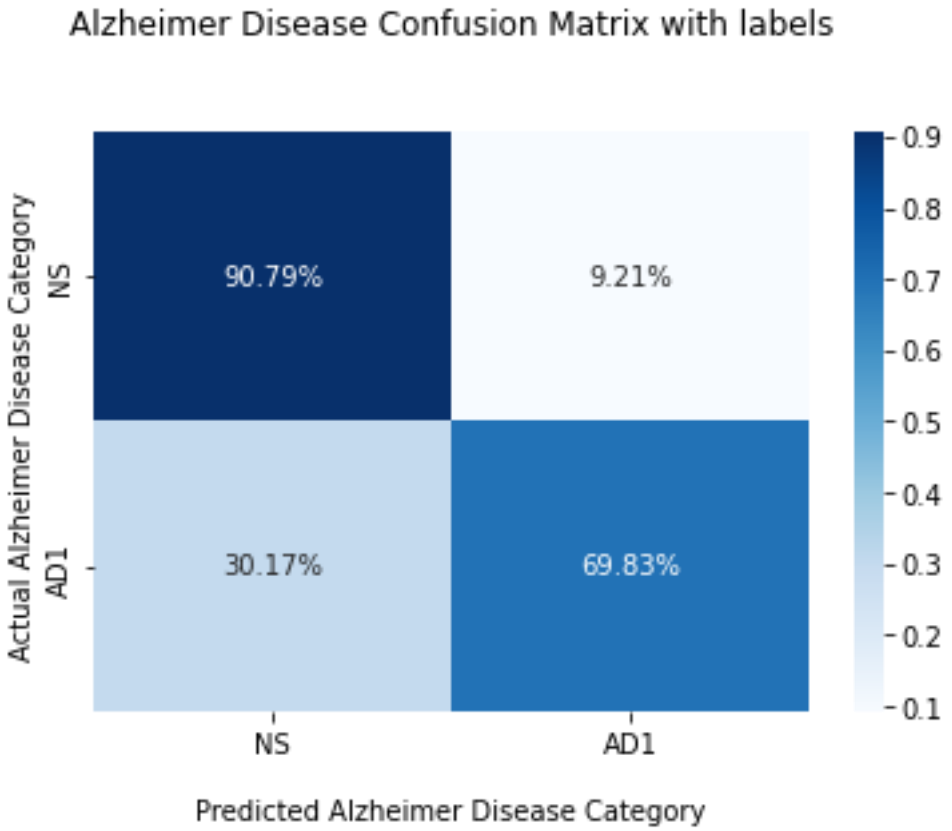

Figure 39: Fp2 channel NS and AD1 Confusion Matrix

Accuracy = 0. 8171641791044776

Sensitivity = 0. 6982758620689655

Specificity = 0. 9078947368421053

The data of the Fp2 channel is divided into AD2 and NS. Then, these data were trained and tested with AlexNet deep learning model using Google Colap. Obtained results are presented below.

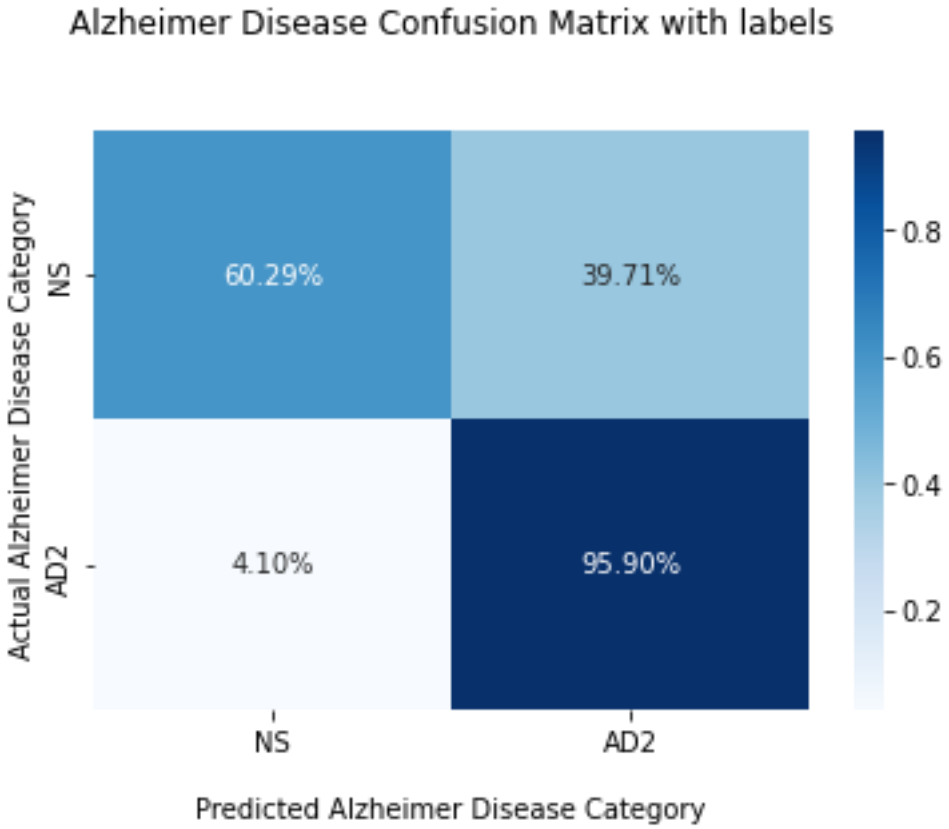

Figure 40: Fp2 channel NS and AD2 Confusion Matrix

Accuracy = 0. 7713178294573644

Sensitivity = 0. 9590163934426229

Specificity = 0. 6029411764705882

7.1.13 EEG Channel F4

The data of the F4 channel is divided into AD1 and NS. Then, these data were trained and tested with AlexNet deep learning model using Google Colap. Obtained results are presented below.

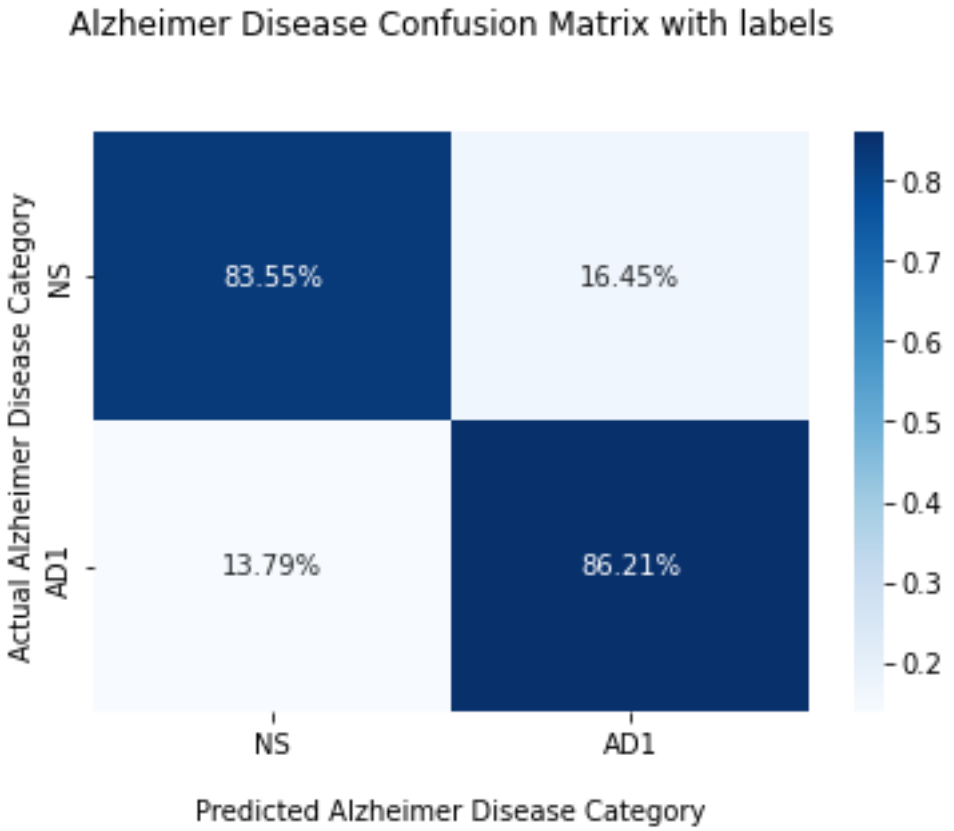

Figure 41: F4 channel NS and AD1 Confusion Matrix

Accuracy = 0. 8470149253731343

Sensitivity = 0. 8620689655172413

Specificity = 0. 8355263157894737

The data of the F4 channel is divided into AD2 and NS. Then, these data were trained and tested with AlexNet deep learning model using Google Colap. Obtained results are presented below.

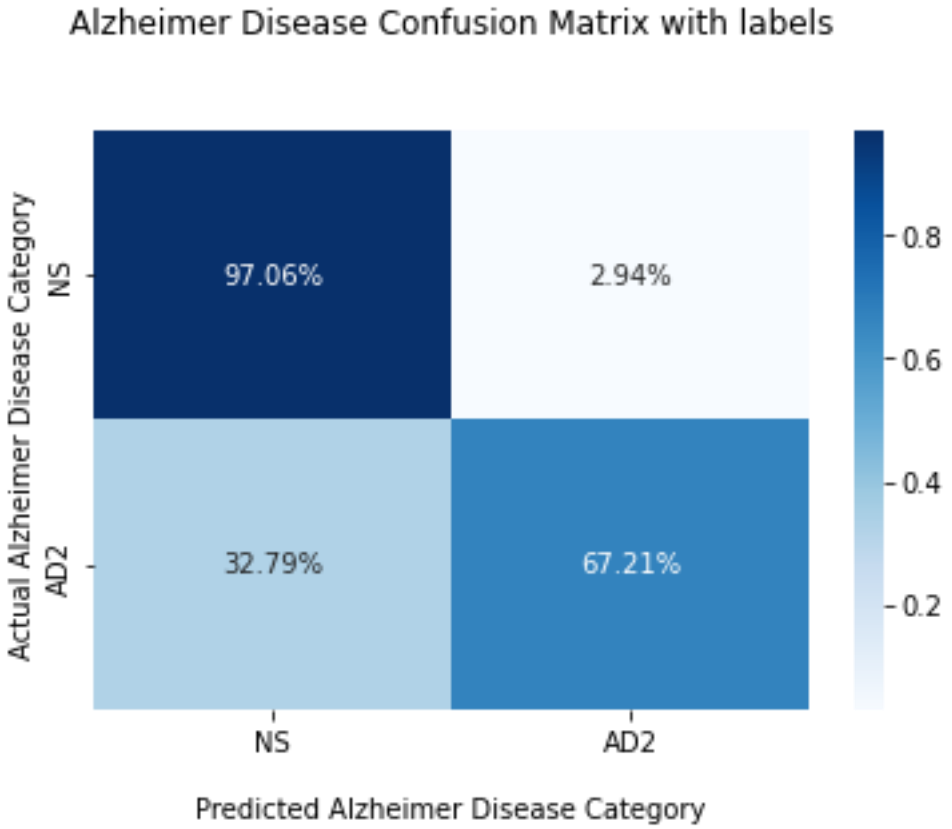

Figure 42: F4 channel NS and AD2 Confusion Matrix

Accuracy = 0. 8294573643410853

Sensitivity = 0. 6721311475409836

Specificity = 0. 9705882352941176

7.1.14 EEG Channel C4

The data of the C4 channel is divided into AD1 and NS. Then, these data were trained and tested with AlexNet deep learning model using Google Colap. Obtained results are presented below.

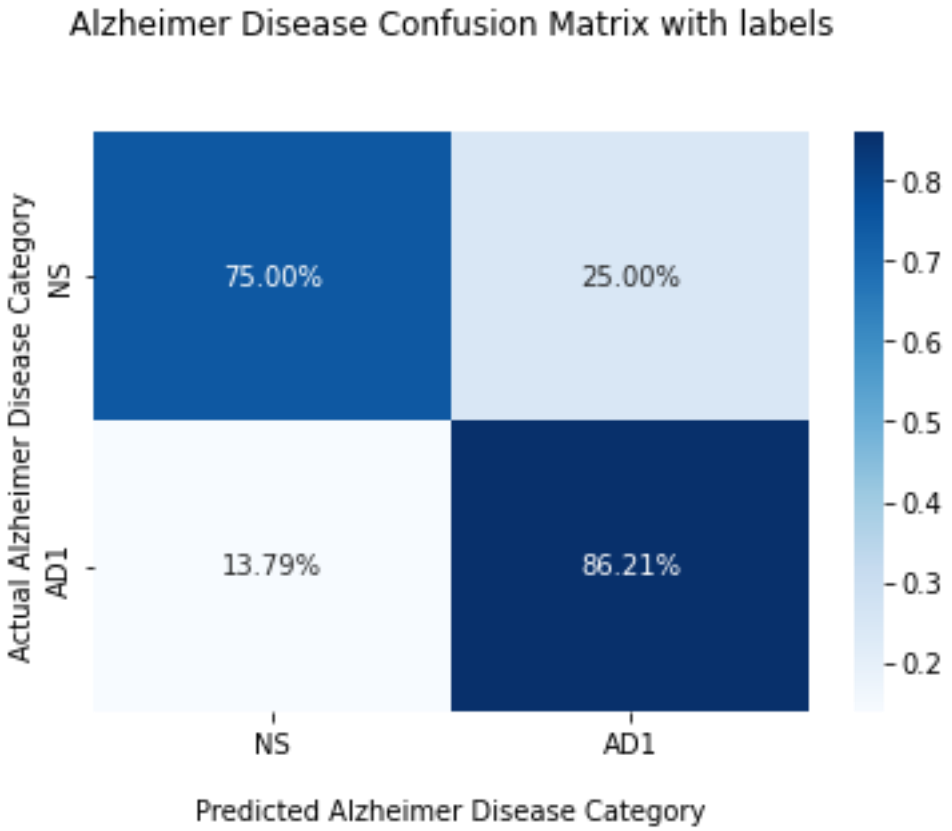

Figure 43: C4 channel NS and AD1 Confusion Matrix

Accuracy = 0. 7985074626865671

Sensitivity = 0. 8620689655172413

Specificity = 0. 75

The data of the C4 channel is divided into AD2 and NS. Then, these data were trained and tested with AlexNet deep learning model using Google Colap. Obtained results are presented below.

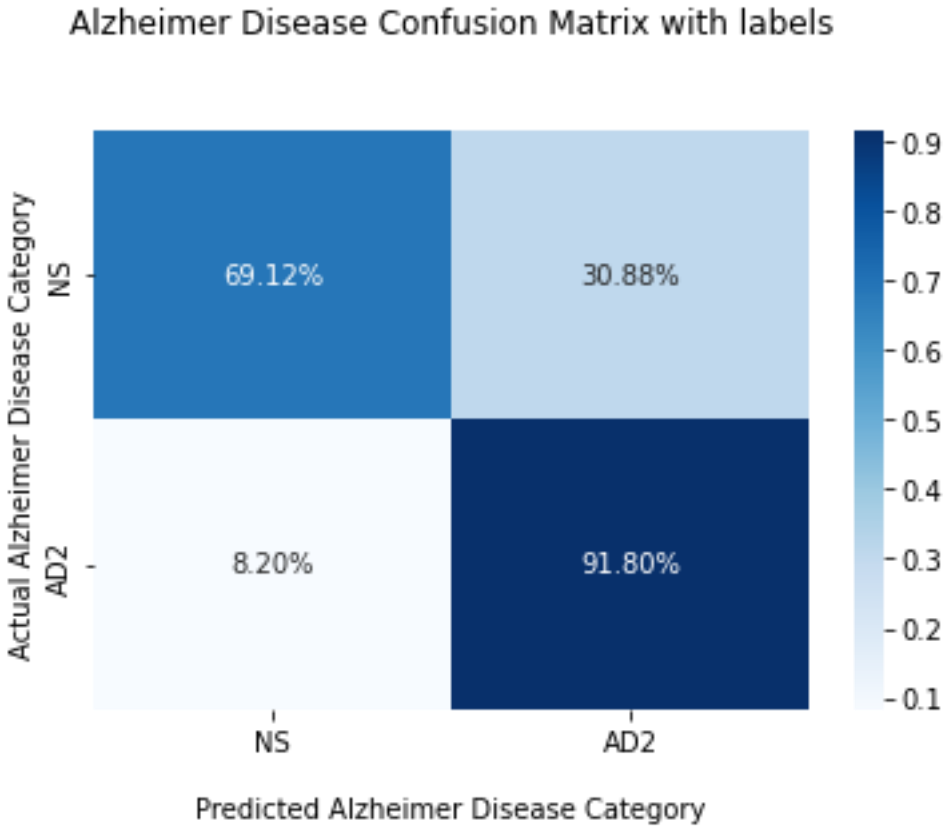

Figure 44: C4 channel NS and AD2 Confusion Matrix

Accuracy = 0. 7984496124031008

Sensitivity = 0. 9180327868852459

Specificity = 0. 6911764705882353

7.1.15 EEG Channel P4

The data of the P4 channel is divided into AD1 and NS. Then, these data were trained and tested with AlexNet deep learning model using Google Colap. Obtained results are presented below.

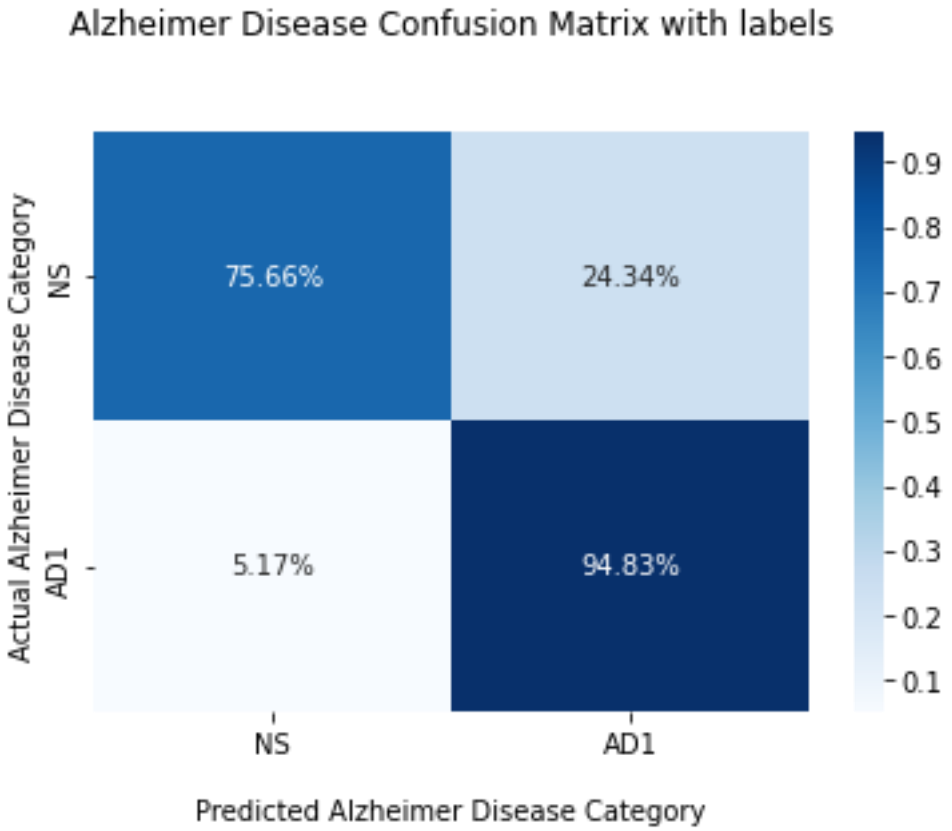

Figure 45: P4 channel NS and AD1 Confusion Matrix

Accuracy = 0. 8395522388059702

Sensitivity = 0. 9482758620689655

Specificity = 0. 756578947368421

The data of the P4 channel is divided into AD2 and NS. Then, these data were trained and tested with AlexNet deep learning model using Google Colap. Obtained results are presented below.

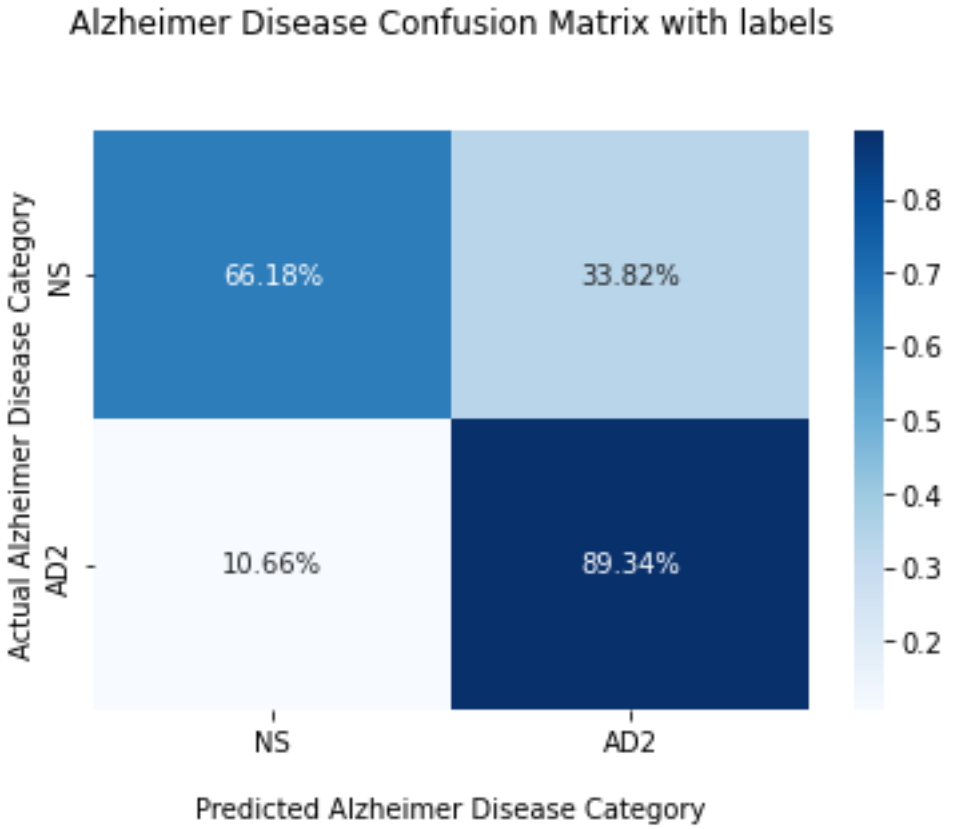

Figure 46: P4 channel NS and AD2 Confusion Matrix

Accuracy = 0. 7713178294573644

Sensitivity = 0. 8934426229508197

Specificity = 0. 6617647058823529

7.1.16 EEG Channel O2

The data of the O2 channel is divided into AD1 and NS. Then, these data were trained and tested with AlexNet deep learning model using Google Colap. Obtained results are presented below.

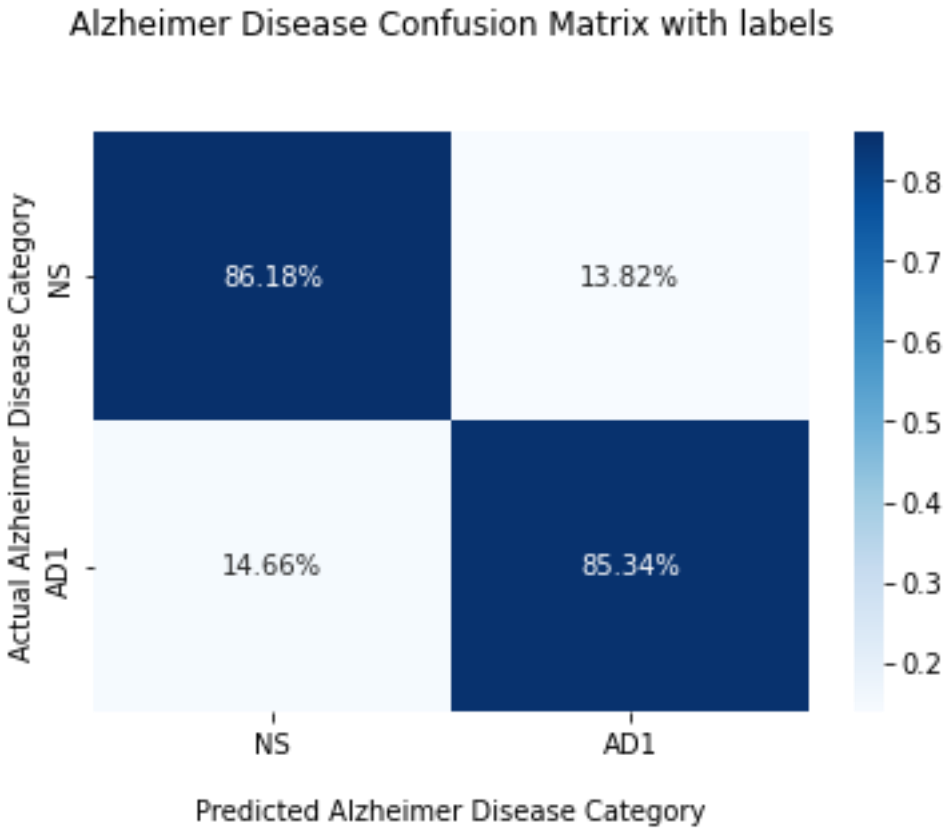

Figure 47: O2 channel NS and AD1 Confusion Matrix

Accuracy = 0. 8582089552238806

Sensitivity = 0. 853448275862069

Specificity = 0. 8618421052631579

The data of the O2 channel is divided into AD2 and NS. Then, these data were trained and tested with AlexNet deep learning model using Google Colap. Obtained results are presented below.

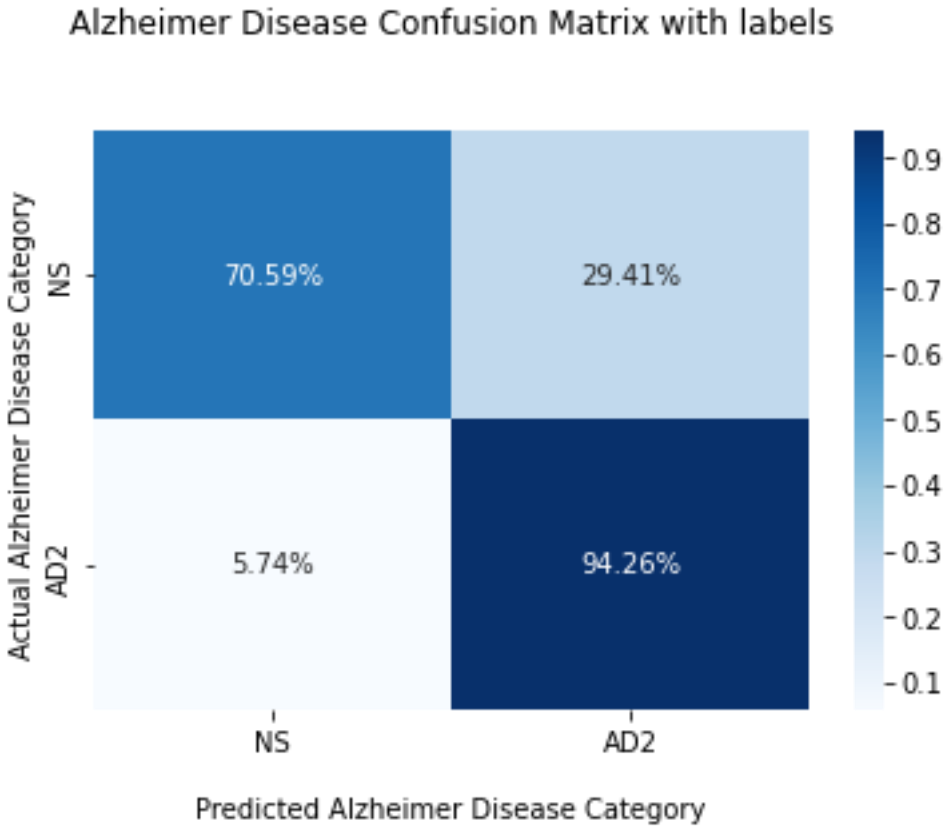

Figure 48: O2 channel NS and AD2 Confusion Matrix

Accuracy = 0. 8178294573643411

Sensitivity = 0. 9426229508196722

Specificity = 0. 7058823529411765

7.2 General Results

All channels are individually trained and tested using Google Colab. Obtained results are presented below.

Table 3: Results of all channels

Channel	AD1			AD2		
	Accuracy	**Sensitivity**	**Specificity**	**Accuracy**	**Sensitivity**	**Specificity**
F7	0.88	0.84	0.92	0.93	0.80	0.87
T3	0.86	0.81	0.90	0.86	0.89	0.84
T5	0.86	0.81	0.90	0.85	0.77	0.95
Fp1	0.78	0.52	0.98	0.60	0.98	0.25
F3	0.86	0.84	0.88	0.81	0.82	0.80
C3	0.86	0.76	0.93	0.77	0.96	0.60
P3	0.76	0.62	0.88	0.84	0.91	0.77
O1	0.79	0.88	0.73	0.84	0.81	0.86
F8	0.79	0.90	0.70	0.82	0.68	0.98
T4	0.79	0.70	0.86	0.70	0.97	0.47
T6	0.83	0.82	0.83	0.77	0.54	0.97
Fp2	0.81	0.69	0.90	0.77	0.95	0.60
F4	0.84	0.86	0.83	0.82	0.67	0.97
C4	0.79	0.86	0.75	0.79	0.91	0.69
P4	0.83	0.94	0.75	0.77	0.89	0.99
O2	0.85	0.85	0.86	0.81	0.94	0.70

All channels are individually trained and tested with Google Colab. It has been observed that a maximum of 3 channels can be run simultaneously with the Google colab GPU memory. For this reason, it was desired to conduct training and testing by selecting the 3 channels with the highest results. In the results obtained, it was seen that the highest results were obtained in the T3, F7 and T5 channels. Therefore, the data from these 3 channels were combined into a single file.

A single NS file is obtained by combining the NS files of 3 channels. This is also done for AD1 and AD2. GPU memory is insufficient when using k-fold cross validation for better results when running the model. To apply K-fold Cross Validation, 20,000 images were randomly selected from each file (NS, AD, AD2) to minimize data in the 3 selected channels. The resulting file contains a total of 60,000 images. It allows 60000 images to work without exceeding the memory capacity of the system.

Results are presented in 2 different ways. The first of these was achieved using only NS and AD1. The latter was obtained using NS and AD2.

All the same processes were trained and tested in K-Fold Cross Validation. All results are listed below.

Data from T3, F7 and T5 channels for NS and AD1 were trained and tested using AlexNet and Google Colab's deep learning model. Obtained results are presented below.

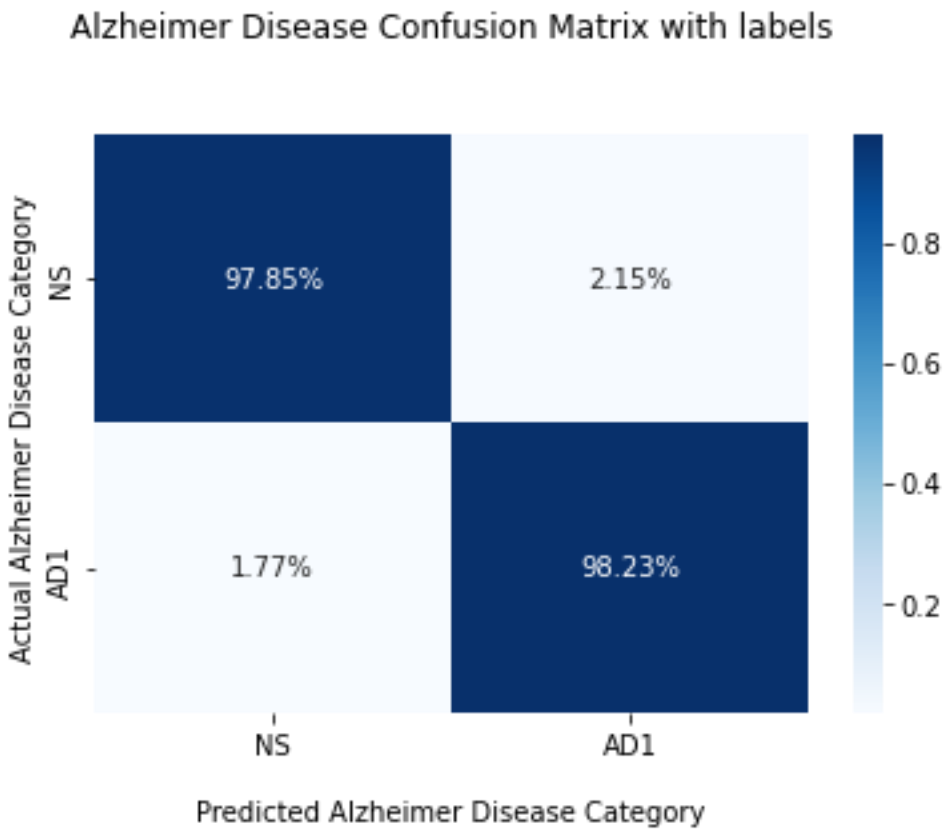

Figure 49: T3, F7, T5 channel NS and AD1 Confusion Matrix

Accuracy = 0.9803970533150206

Sensitivity = 0.9823119083208769

Specificity = 0.9784730913642052

Data from T3, F7 and T5 channels for NS and AD2 were trained and tested using AlexNet and Google Colab's deep learning model. Obtained results are presented below.

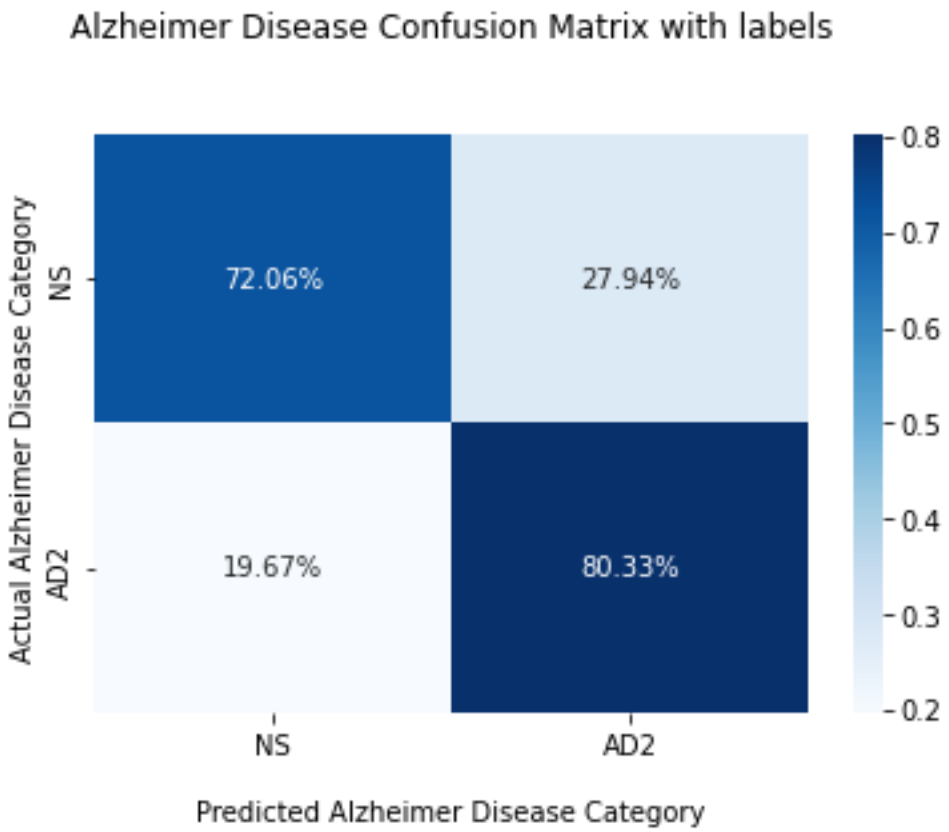

Figure 50: T3, F7, T5 channel NS and AD2 Confusion Matrix

Accuracy = 0.7596899224806202

Sensitivity = 0.8032786885245902

Specificity = 0.7205882352941176

7.2.1 General Results With K-Fold

K-Fold Cross Validation was used to get better results.[28] Google Colab's gpu capacity is suitable for 4-Fold at most. Therefore, the model was trained and tested along 4-Fold using K-Fold Cross Validation. This was done using the T3, F7, T5 channel data for NS and AD1. Obtained results are presented below.

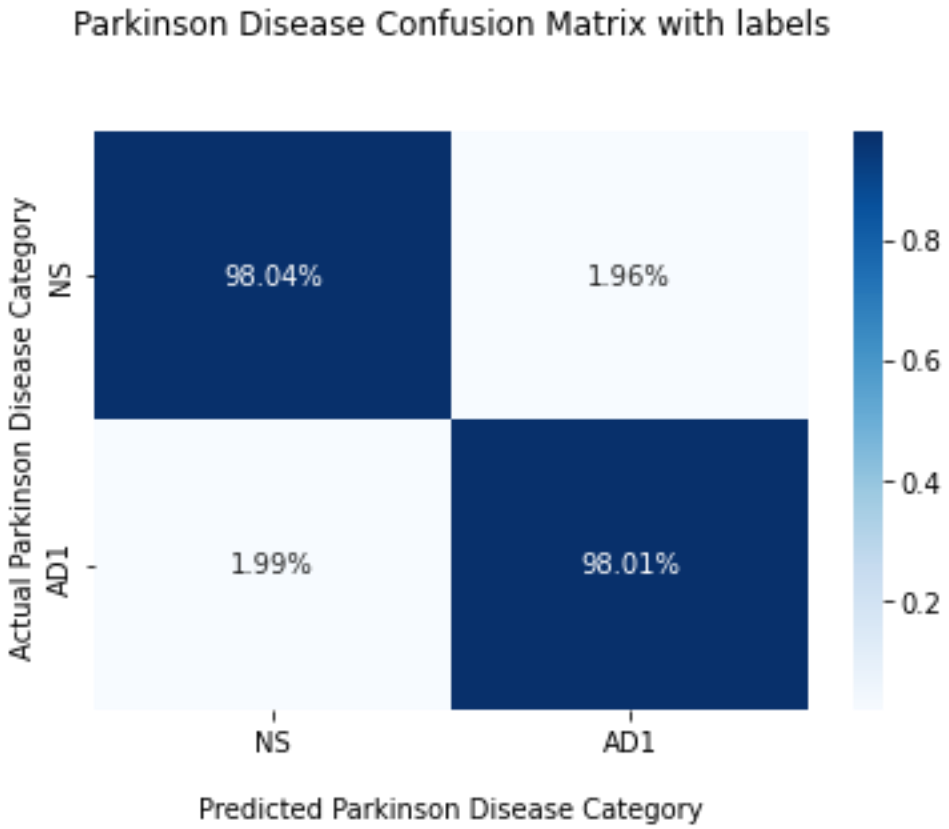

Figure 51: T3, F7, T5 channel NS and AD1 Confusion Matrix

Accuracy = 0.9802721937819953

Sensitivity = 0.980110775427996

Specificity = 0.9804310131285608

K-Fold Cross Validation was used to get better results.[28] Google Colab's gpu capacity is suitable for 4-Fold at most. Therefore, the model was trained and tested along 4-Fold using K-Fold Cross Validation. This was done using the T3, F7, T5 channel data for NS and AD2. Obtained results are presented below.

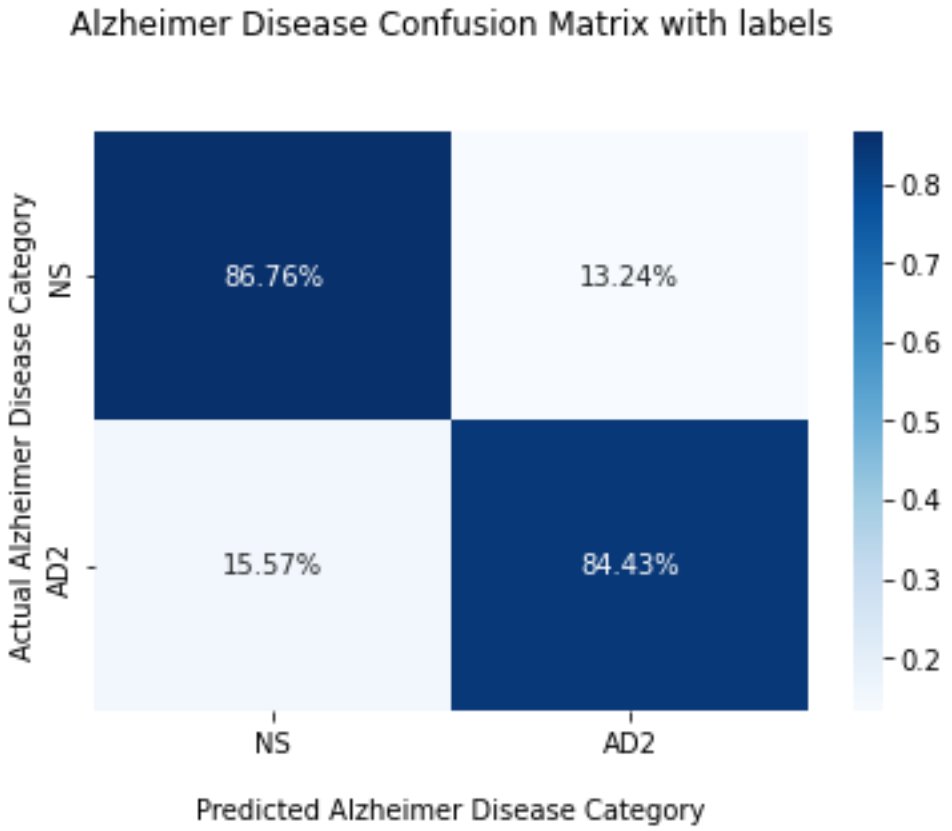

Figure 52: T3, F7, T5 channel NS and AD2 Confusion Matrix

Accuracy = 0.8565891472868217

Sensitivity = 0.8442622950819673

Specificity = 0.8676470588235294

7.3 Discussion

All obtained results were compared with similar studies conducted in recent years. The following comparison table, the neural network used in the studies and the results obtained are presented in the table below.

Table 4: Results and other studies

Authors	Year	Techniques	Accuracy
Kulkarni et al[29]	2017	SVM	96
Bairagi[30]	2018	SVM	94
Ruiz-Gómez et al [31]	2018	MLP	78.43
Kulkarni[32]	2018	KNN	94
Amezquita-Sanche et al[33]	2019	EPPN	90.3
Uğur's Work	2022	CNN	98.03
Uğur's Work with K-Fold	2022	CNN	98.02

Two different results were obtained in this study. Although there is little difference between the results obtained, the 4-model model gave higher results. There are many studies using different techniques and different neural networks in the early diagnosis of Alzheimer's disease. Although CNN was used in most of these studies, ANN, LSSVM, SVM, MLP, KNN and RNN neural network models were also used, unlike CNN. The table above presents the studies conducted in this field and the results of these studies. The GASF technique we used and the deep CNN model gave a very high result with 98.02. When compared with other studies in this field, it was seen that the GASF technique and CNN deep network used gave higher results than most of the

other studies. However, it has been observed that there are more successful studies in this area.

Chapter 8

CONCLUSION

Alzheimer's disease has no cure. However, the progression of Alzheimer's disease can be slowed down with drug therapy. Alzheimer's disease consists of 5 stages. Therefore, it is very important to diagnose Alzheimer's disease before its stages progress and to start drug therapy to slow the progression of the disease. Alzheimer's disease can only be diagnosed by a neurologist. In this study, it is aimed to diagnose Alzheimer's disease in the early stages with artificial intelligence.

As a result, in this study, it is aimed to classify 2D images with AlexNet CNN model by using GASF technique for early diagnosis of Alzheimer's disease. The results obtained are promising. Although the success of the CNN model was proven in 2D images, it was not known how successful it was in classifying GASF images. This study has proven that the GASF technique is at least as successful as the techniques in other studies.

When the results were examined, satisfactory results were obtained with the AlexNet CNN model with 98.02% Accuracy, 98.01% Sensitivity and 98.04% Specificity.

Chapter 9

IN THE FUTURE

In this study, the deep learning model was trained and tested by creating 2D images with the Gramian Angular Summation Field (GASF) technique. In the future, it is predicted that Gramian Angular Difference Field (GADF) and Markov Transition Fields (MTF) techniques such as GASF can be used to obtain higher results than these obtained results.

In addition, although the CNN model was successful in examining the 2D drawing, it was observed that higher results could be obtained with RNN based on some of the literature. It is predicted that high results can be obtained by using RNN neural network instead of CNN in the future.

REFERENCES

[1] Bairagi, V. (2018). EEG signal analysis for early diagnosis of Alzheimer disease using spectral and wavelet based features. *International Journal of Information Technology*, *10*(3), 403-412.

[2] Trambaiolli, L. R., Spolaôr, N., Lorena, A. C., Anghinah, R., & Sato, J. R. (2017). Feature selection before EEG classification supports the diagnosis of Alzheimer's disease. *Clinical Neurophysiology*, *128*(10), 2058-2067.

[3] Blank, R. H. (2019). Alzheimer's disease and other dementias: an introduction. In *Social & Public Policy of Alzheimer's Disease in the United States* (pp. 1-26). Palgrave Pivot, Singapore.

[4] Huggins, C. J., Escudero, J., Parra, M. A., Scally, B., Anghinah, R., De Araújo, A. V. L., ... & Abasolo, D. (2021). Deep learning of resting-state electroencephalogram signals for three-class classification of Alzheimer's disease, mild cognitive impairment and healthy ageing. *Journal of Neural Engineering*, *18*(4), 046087.

[5] Fiscon, G., Weitschek, E., Felici, G., Bertolazzi, P., De Salvo, S., Bramanti, P., & De Cola, M. C. (2014, December). Alzheimer's disease patients classification through EEG signals processing. In *2014 IEEE Symposium on Computational Intelligence and Data Mining (CIDM)* (pp. 105-112). IEEE.

[6] Zhao, Y., & He, L. (2014, November). Deep learning in the EEG diagnosis of Alzheimer's disease. In *Asian conference on computer vision* (pp. 340-353). Springer, Cham.

[7] Acharya, U. R., Oh, S. L., Hagiwara, Y., Tan, J. H., & Adeli, H. (2018). Deep convolutional neural network for the automated detection and diagnosis of seizure using EEG signals. *Computers in biology and medicine*, *100*, 270-278.

[8] Lacko, D. (2017). The application of 3D anthropometry for the development of headgear-a case study on the design of ergonomic brain-computer interfaces.

[9] Wikimedia Foundation. (2022, March 13). 10–20 system (EEG). Wikipedia. Retrieved July 20, 2022, from https://en.wikipedia.org/wiki/10%E2%80%9320_system_%28EEG%29

[10] Ramakrishnan, A. G., & Satyanarayana, J. V. (2016). Reconstruction of EEG from limited channel acquisition using estimated signal correlation. *Biomedical Signal Processing and Control*, 27, 164-173.

[11] Krizhevsky, A., Sutskever, I., & Hinton, G. E. (2012). Imagenet classification with deep convolutional neural networks. *Advances in neural information processing systems*, 25.

[12] Han, X., Zhong, Y., Cao, L., & Zhang, L. (2017). Pre-trained alexnet architecture with pyramid pooling and supervision for high spatial resolution remote sensing image scene classification. *Remote Sensing*, 9(8), 848.

[13] LeCun, Y., Bottou, L., Bengio, Y., & Haffner, P. (1998). Gradient-based learning applied to document recognition. *Proceedings of the IEEE*, 86(11), 2278-2324.

[14] Feng, J., He, X., Teng, Q., Ren, C., Chen, H., & Li, Y. (2019). Reconstruction of porous media from extremely limited information using conditional generative adversarial networks. *Physical Review E*, *100*(3), 033308.

[15] Wang, Z., & Oates, T. (2015, June). Imaging time-series to improve classification and imputation. *In Twenty-Fourth International Joint Conference on Artificial Intelligence.*

[16] Refaeilzadeh, P., Tang, L., & Liu, H. (2009*). Cross-validation. Encyclopedia of database systems*, 5, 532-538.

[17] Kanda, P. A. M., Trambaiolli, L. R., Lorena, A. C., Fraga, F. J., Basile, L. F. I., Nitrini, R., & Anghinah, R. (2014). Clinician's road map to wavelet EEG as an Alzheimer's disease biomarker. *Clinical EEG and neuroscience*, *45*(2), 104-112.

[18] Fraga, F. J., Falk, T. H., Trambaiolli, L. R., Oliveira, E. F., Pinaya, W. H., Kanda, P. A., & Anghinah, R. (2013, May). Towards an EEG-based biomarker for Alzheimer's disease: Improving amplitude modulation analysis features. In *2013*

IEEE International Conference on Acoustics, Speech and Signal Processing (pp. 1207-1211). IEEE.

[19] Cassani, R., Falk, T. H., Fraga, F. J., Kanda, P. A., & Anghinah, R. (2014, May). Towards automated EEG-Based Alzheimer's disease diagnosis using relevance vector machines. In *5th ISSNIP-IEEE Biosignals and Biorobotics Conference (2014): Biosignals and Robotics for Better and Safer Living (BRC)* (pp. 1-6). IEEE).

[20] Merlin Praveena, D., Angelin Sarah, D., & Thomas George, S. (2020). Deep learning techniques for EEG signal applications–a review. *IETE Journal of Research*, 1-8.

[21] Oh, S. L., Hagiwara, Y., Raghavendra, U., Yuvaraj, R., Arunkumar, N., Murugappan, M., & Acharya, U. R. (2020). A deep learning approach for Parkinson's disease diagnosis from EEG signals. *Neural Computing and Applications*, 32(15), 10927-10933.

[22] Shaban, M. (2021, May). Automated screening of parkinson's disease using deep learning based electroencephalography. *In 2021 10th International IEEE/EMBS Conference on Neural Engineering (NER)* (pp. 158-161). IEEE.

[23] Vanegas, M. I., Ghilardi, M. F., Kelly, S. P., & Blangero, A. (2018, December). Machine learning for EEG-based biomarkers in Parkinson's disease. *In 2018*

IEEE International Conference on Bioinformatics and Biomedicine (BIBM) (pp. 2661-2665). IEEE.

[24] Cahoon, S., Khan, F., Polk, M., & Shaban, M. (2021, December). Wavelet-based convolutional neural network for parkinson's disease detection in resting-state electroencephalography. *In 2021 IEEE Signal Processing in Medicine and Biology Symposium (SPMB)* (pp. 1-5). IEEE.

[25] Alnajjar, M. (2021). Image-based detection using deep learning and google colab. *International Journal of Academic Information Systems Research*, *5*(1), 30–35.

[26] Hussain, S., Dixit, P., & Hussain, M. S. (2020). Image processing in artificial intelligence. *International Journal of Scientific Research in Computer Science, Engineering and Information Technology*, *6*(1), 244-249.

[27] Marques, L., Lopes, L., Ferreira, M., Wanzeller, C., Martins, P., & Abbasi, M. (2022). Image processing: impact of train and test sizes on custom image recognition algorithms. In *Marketing and Smart Technologies* (pp. 365-380). Springer, Singapore.

[28] Refaeilzadeh, P., Tang, L., & Liu, H. (2009*). Cross-validation. Encyclopedia of database systems*, 5, 532-538.

[29] Kulkarni, N. N., & Bairagi, V. K. (2017). Extracting salient features for EEG-based diagnosis of Alzheimer's disease using support vector machine classifier. *IETE Journal of Research*, *63*(1), 11-22.

[30] Trambaiolli, L. R., Spolaôr, N., Lorena, A. C., Anghinah, R., & Sato, J. R. (2017). Feature selection before EEG classification supports the diagnosis of Alzheimer's disease. *Clinical Neurophysiology*, *128*(10), 2058-2067.

[31] Ruiz-Gómez, S. J., Gómez, C., Poza, J., Gutiérrez-Tobal, G. C., Tola-Arribas, M. A., Cano, M., & Hornero, R. (2018). Automated multiclass classification of spontaneous EEG activity in Alzheimer's disease and mild cognitive impairment. *Entropy*, *20*(1), 35.

[32] Kulkarni, N. (2018). Use of complexity based features in diagnosis of mild Alzheimer disease using EEG signals. *International Journal of Information Technology*, *10*(1), 59-64.

[33] Amezquita-Sanchez, J. P., Mammone, N., Morabito, F. C., Marino, S., & Adeli, H. (2019). A novel methodology for automated differential diagnosis of mild cognitive impairment and the Alzheimer's disease using EEG signals. *Journal of neuroscience methods*, *322*, 88-95.